Gravitational lensing by damped Ly-α absorbers

Alain Smette

Kapteyn Astronomical Institute, Postbus 800, NL-9700 AV Groningen, The Netherlands, email: asmette@astro.rug.nl; fax: +31-50-3636100

Jean-François Claeskens

Institut d'Astrophysique, Université de Liège, Avenue de Cointe 5, B-4000 Liège, Belgium, Research Assistant, Belgian Fund for Scientific Research (FNRS), claesken@astro.ulg.ac.be, fax: +32-4-2527474

Jean Surdej

Space Telescope Science Institute, 3700 San Martin Drive, Baltimore MD 21218, USA, presently member of the Astrophysics Division, Space Science Department of the European Space Agency, also, Research Director, Belgian Fund for Scientific Research (FNRS), surdej@astro.ulg.ac.be, fax: +32-4-2527474

Abstract

Assuming that (i) damped Ly-α absorbers (DLAs) arise in present-day-like spiral galaxies which are immersed in isothermal dark matter halos, (ii) that these galaxies obey the Tully-Fisher $\sigma/\sigma_* = (L/L_*)^{1/\alpha_{\rm TF}}$ and the Holmberg $R_{\rm L}/R_* = (L/L_*)^{\alpha_{\rm H}}$ relations, and (iii) that they follow the Schechter luminosity distribution, we describe how their observed number density ($d\mathcal{N}/dz$), distribution of column density ($f(N)$) as well as inferred cosmological density of H I ($\Omega_{\rm HI}$) derived from DLA surveys are affected by gravitational lensing (GL). The 'by-pass' effect causes the lines-of-sight (LOSs) towards background QSOs to avoid the central parts of galaxies and reduces their effective cross-section for absorption; the 'amplification bias' leads observers to select QSOs whose LOSs preferentially cross galaxies close to their Einstein radius. As a consequence, the determination of the quantities $d\mathcal{N}/dz$, $f(N)$ and $\Omega_{\rm HI}$ from DLA surveys does not only depend on the redshift z and luminosity L of galaxies responsible for the absorbers but also on the column density profile of H I within the galaxies and on the redshift $z_{\rm q}$ and magnitude $b_{\rm q}$ of the background QSOs.

For most of the existing surveys using $b_{\rm q} \lesssim 19$ QSOs, the amplification bias dominates the combined effect resulting in a slight overestimate of $d\mathcal{N}/dz$, $f(N)$ and

$\Omega_{\rm HI}$. We mainly find that observational strategies presently used to produce high-z DLA surveys result in avoiding the signature of significant GL effects: following our model, we determine that an overestimate of $\Omega_{\rm HI}$ by more than 10% is unlikely for the $z > 1.7$ existing surveys, but may reach $\simeq 35\%$ for the low redshift ones.

However, we show that, in the absence of extinction by dust and micro-lensing effects, surveys ideally designed to enhance GL effects, i.e. to search for DLAs at $z \sim 0.5$ in front of very bright ($b_{\rm q} \simeq 16$), high-z ($z_{\rm q} > 1$) QSOs, may lead 1) to overestimate by up to $\simeq 90\%$ the number of DLAs per unit redshift; 2) to bias the survey towards high H I column density systems so that it could contain up to 4 times as many such systems, thus 3) to overestimate by up to $\simeq 170\%$ the cosmological density of gas associated with those DLAs. Identification of the galaxies responsible for the DLAs may be severely biased towards luminous galaxies if $2/\alpha_{\rm TF} - \alpha_{\rm H} > 0$; this latter effect is greatly increased for $\log N_{\rm HI} > 21$ DLAs.

Hence, GL effects on the quantities derived from surveys for $z \sim 0.5$ DLAs are of the same order, but of opposite direction, as the effects of extinction by dust (cf. Fall & Pei 1993). However, the GL and dust extinction effects do not compensate each other: combining them in a consistent way is necessary to interpret existing DLA surveys. Furthermore, the effects due to micro-lensing should be simultaneously taken into account. We intend to report the results on the complex interplay between macro-lensing, micro-lensing and dust in a subsequent paper.

We briefly present statistical tests specifically designed to check whether GL affects existing DLA surveys, and assuming that extinction by dust is negligible. We only find indications of GL effects for the $z < 1$ ones which, if confirmed, might even be stronger than predicted by our model.

We show that an independent work on the same subject by Bartelmann & Loeb (1996) incorrectly treats the inclination effects for the intervening galaxies, thus undermining some of their main results and conclusions.

Keywords: galaxies: evolution, gravitational lensing, quasars: absorption lines
PACS code: 98.80.Es, 98.62.S, 98.62.Ai

1 Introduction

Systems showing damped Ly-α absorption lines (hereafter, DLAs) in quasar spectra are thought to arise in the progenitors of present-day disk galaxies (Wolfe 1988). Following customary uses, a DLA is defined as a system presenting a neutral hydrogen column density $N_{\rm DLA} \geq 2\ 10^{20}$ cm^{-2}. This approximately corresponds to the column density measured at the optical radius $R_{\rm L}$ of local spiral galaxies.

Recent studies (Lanzetta, Wolfe and Turnshek 1995, hereafter LWT) show that DLAs contain at least a large fraction, if not all, of the H I content of the Universe at high-z. Furthermore, the cosmological mass density ($\Omega_{\rm HI}$) of H I to which they are associated at $z \approx 3.5$ appears to be similar to the one

(Ω_s) contained in stars at $z = 0$, so that their quantity of H I may have been sufficient to form the entire stellar content of nearby galaxies. The variation of Ω_{HI} with z thus provides an indication of the change in the overall rate of star formation in the Universe.

These results are based on the assumption that *the lines-of-sight* (hereafter, LOSs) *towards background quasars are randomly distributed over the sky*, in particular, that *they are unaffected by the DLAs themselves*. However, gravitational lensing (hereafter GL) potentially undermines this assumption as a result of (Smette 1995):

- the 'by-pass' effect: a random LOS has its effective impact parameter R increased relatively to the unlensed case; the central part of a galaxy is thus avoided and LOSs that would go through the outskirts of a spiral galaxy may very well cross the disk outside the optical radius; this effect is a natural consequence of the 'convergence' of a GL;
- the 'amplification bias': a significant fraction of QSOs selected from flux limited samples have their apparent magnitude b_q boosted by GL amplification, thus increasing the relative number of QSOs with DLAs in such samples (Surdej 1990).

In the following, we derive some consequences of these two effects and design statistical tests in order to check whether GL actually affects existing surveys of DLAs and published estimates of Ω_{HI}. In the remainder, we assume that $H_0 = 100\ h$ km s^{-1} Mpc^{-1}, but most of the results are independent of H_0. Similarly, we assume that $q_0 = 1/2$ and $\Lambda = 0$, except when mentioned otherwise.

It is important to realize that extinction by dust may also play an important role in the selection of LOSs towards background quasars, as emphasized by Fall & Pei (1993): its effect on values derived from DLA surveys is *a priori* opposite to the amplification bias due to gravitational lensing, leading to underestimate very high-column density systems. However, Sec. 5.6 briefly describes how the combination of the two effects may lead to counter-intuitive consequences.

In order to estimate the influence of lensing alone, we shall however neglect extinction by dust in the present work. We also neglect possible micro-lensing effects arising in the DLAs, that may lead to another contribution to the amplification bias. Furthermore, we assume that the galaxies associated with DLAs are the only objects located along the LOSs towards background quasars, and that they lie in an otherwise homogeneous density universe.

Most of the assumptions that we use here are common or very similar to those in the independent work carried on by Bartelmann & Loeb (1996). However, their treatment of the inclination effects for the intervening galaxies contains a fundamental error which is explained in Sec 4.7.

The models for present-day spiral galaxies used in this study are introduced in Sec. 2. Section 3 describes the formalism we have developed to take into account the gravitational lensing effects. Their influence on the determination of $d\mathcal{N}/dz$, $f(N)$ and $\Omega_{\rm HI}$ as derived from DLA surveys are presented in Sec. 4. We list in Sec. 5 a number of caveats to the present model which may affect the results we have obtained. Some observational aspects and statistical tests relevant to the effects of lensing on existing DLA surveys are presented in Sec. 6. Main conclusions are summarized in Sec. 7.

2 Models of present-day spiral galaxies

In order to evaluate the effects of gravitational lensing, we need a model for the spiral galaxies which we assume contain the H I layer responsible for the DLA lines. Such a model must provide: (1) the spatial extent of these galaxies in order to compute their cross-section for DLA absorption; (2) their surface density profile for the evaluation of their lensing properties; (3) their H I column density profile and number density per unit volume for the derivation of the H I column density distribution. It fortunately appears that all these quantities may be related to the galaxy luminosity function.

2.1 Model of spiral galaxies

We consider that spiral galaxies obey the Tully-Fisher relation (Tully & Fisher 1977)

$$\sigma = \sigma_* \left(\frac{L}{L_*}\right)^{1/\alpha_{\rm TF}} , \tag{1}$$

with $\sigma = v_{\rm max}/\sqrt{2}$, $v_{\rm max}$ being the maximal value of the rotational velocity of a galaxy with luminosity L. We adopt the values $\sigma_* = 144$ km s^{-1}, $M_*(B_{\rm T}^0) = -19.9$ and $\alpha_{\rm TF} = 2.6$, in accordance with Fukugita and Turner's study (1991).

We assume that the galaxy optical radii $R_{\rm L}$ follow the Holmberg's radius-luminosity relation

$$R_{\rm L} = R_* \left(\frac{L}{L_*}\right)^{\alpha_{\rm H}} . \tag{2}$$

The Holmberg radius for a L_* galaxy is $R_* = 11\ h^{-1}$ kpc and the exponent $\alpha_{\rm H} = 5/12$ (Holmberg 1975).

We consider that the spiral galaxies are embedded in dark matter halos which are reasonably well described by a Singular Isothermal Sphere (SIS), characterized by the one-dimensional velocity dispersion $\sigma_{\rm SIS} = \sigma$. Adopting an axis-symmetric lens considerably simplifies the subsequent mathematical treatment. The SIS lens model approximates very well the lensing properties of real galaxies except for light rays passing very near and far away from the center. However, for statistical purposes, this approximation is essentially good [1] .

2.2 Models of the column density profile

We then assume that the neutral hydrogen is located in a disk with negligible thickness. In order to evaluate the dependence of the lensing effects on the column density profile within the galaxy, we shall consider two distinct models. The first model is relatively simple as it is just an exponentially decreasing column density profile; the second model is more realistic and takes into account a decrease in the H I distribution of gas near the center as observed for a large fraction of spiral galaxies.

2.2.1 The exponential model

The first model for the column density profile is based on observations of 50 galaxies obtained by Broeils & van Woerden (1994) and was used by Bartelmann & Loeb (1996). These galaxies were part of a search for spirals with large H I disks to measure their rotation curves at large radii. Consequently, their selection criteria are far from ideal for a precise determination of the column density distribution inside the galaxies, as for example, their inclination had to be larger than 40°.

The inferred (face-on) H I distribution corresponds to the exponential (hereafter E) model:

$$N_{\rm HI}(r, i = 0) = 1.124\ 10^{21}\ 10^{-r/2}\ {\rm cm}^{-2}, \tag{3}$$

where r represents the ratio between the distance to the center of the galaxy R and the optical radius $R_{\rm L}$.

[1] Note that the third lensed image which would appear in non-singular isothermal lens models is usually also very weak and difficult to detect; as a consequence, the SIS lens model is appropriate for our purpose.

In this relation, the maximal column density value for a face-on galaxy is obviously obtained at $r(N_{\rm HI}^{\rm max}) = 0$, for which $N_{\rm HI}^{\rm max} \simeq 1.1\ 10^{21}$ cm^{-2}. The column density at the optical radius for a face-on galaxy is $N_{\rm HI}(r = 1) = 3.5\ 10^{20}$ cm^{-2}. On the other hand, the maximal impact parameter $R_{\rm DLA} = r_{\rm DLA}\ R_{\rm L}$ for producing a DLA in a face-on galaxy is 1.5 $R_{\rm L}$.

2.2.2 The exponential plus gaussian hole model

However, it has been noted for a long time (cf. Roberts 1975) that the H I distribution presents a central depression, at least in the well-studied nearby galaxies. The exponential plus Gaussian hole model (hereafter, the E+GH model)

$$N_{\rm HI}(r, i = 0) = 2.10^{21}\ e^{-2.65\ r}\ \left[1 - 0.81\ e^{-12.5 r^2}\right]\ {\rm cm}^{-2} \tag{4}$$

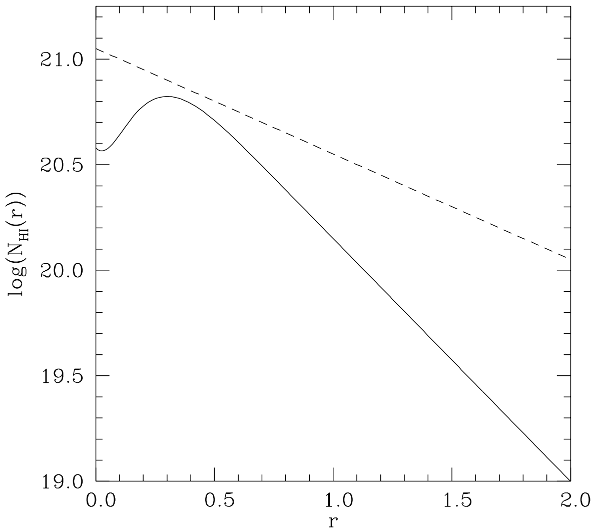

Fig. 1. Neutral hydrogen column density as a function of the impact parameter normalized to the galaxy optical radius $r = R/R_{\rm L}$ for a face-on galaxy, following the exponential + Gaussian hole model given by Eq. 4 (solid) and the exponential model according to Eq. 3 (dash).

represents a fit to the mean of the measured $N_{\rm HI}$ based on H I emission for a complete sample of 27 nearby spiral galaxies (Rao & Briggs 1993), selected to estimate the H I content of the local Universe and thus much more appropriate for our purpose than the Broeils & van Woerden (1994) sample (this relation was kindly provided to us by Frank Briggs). It provides a slightly better fit to the individual H I column density distribution within galaxies than the double Gaussian model adopted by Hewitt, Haynes & Giovanelli (1983). It is important to remember that there is a considerable dispersion in the observed column density around the mean represented in Fig. 1.

Here the maximal column density value for a face-on galaxy is obtained at $r(N_{\rm HI}^{\rm max}) \simeq 0.3$, for which $N_{\rm HI}^{\rm max} \simeq 6.7\ 10^{20}$ cm^{-2}. The column density at the optical radius for a face-on galaxy is here $N_{\rm HI}(r=1) = 1.4\ 10^{20}$ cm^{-2}, less than half the corresponding value for the E model. Similarly, the maximal value of the normalized impact parameter for producing a DLA by a face-on galaxy is $r_{\rm DLA} = 0.87$.

It is apparent from Fig. 1 that the two relations describing the H I column density distribution are very different. One of the purposes of the present study is to investigate whether or not the lensing effects are sensitive to the precise form of the column density profile.

2.3 Luminosity function and number density

We also use the local luminosity function $\Phi(L)$ of spiral galaxies given by Schechter (1976):

$$\Phi\left(\frac{L}{L_*}\right)\ d\left(\frac{L}{L_*}\right) = \Phi_*\ \left(\frac{L}{L_*}\right)^{-\beta}\ e^{-L/L_*}\ d\left(\frac{L}{L_*}\right), \tag{5}$$

with a value of $\beta = 1.1$, which we assume does not evolve with z. On the other hand, we may have an evolving number density Φ_* of spiral galaxies with luminosity L_* per unit comoving volume.

The number density of DLA systems determined at $z = 0$ is $(d\mathcal{N}/dz)_0 = 0.015 \pm 0.004$ (Rao 1994). From Eq. 7 and 8 in Wolfe et al. (1986), one obtains that the local number density of L_* spiral galaxies is

$$\Phi_* = \left(\frac{d\mathcal{N}}{dz}\right)_0\ \left(\frac{11\ h^{-1}\ {\rm kpc}}{r_{\rm DLA}\ R_*}\right)^2\ \frac{1.75\ h^3}{\Gamma(1+2\ \alpha_{\rm H}-\beta)}\ {\rm Mpc}^{-3}, \tag{6}$$

where Γ represents the usual gamma-function, so that: $\Phi_* = 0.028 \pm 0.008\ h^3$ Mpc^{-3} for the E+GH model and $\Phi_* = 0.0094 \pm 0.002\ h^3$ Mpc^{-3} for the E model.

2.4 Evolution of the DLA population

Finally, let us also introduce the evolution parameter γ which describes the dependence of the number density of DLAs per unit redshift as a function of

z, i.e:

$$\frac{d\mathcal{N}}{dz}(z) = \left(\frac{d\mathcal{N}}{dz}\right)_0 (1+z)^\gamma, \tag{7}$$

where $\gamma = 1/2, 1$ corresponds to no evolution if $q_0 = 1/2, 0$, respectively.

Two recent studies lead to contradictory results for a similar redshift range ($0 < z \leq 3.5 - 4$): indeed, Rao, Turnshek & Briggs (1995, hereafter RTB) derived $\gamma = 2.27 \pm 0.25$, which indicates a strong evolution of the product cross-section times the number density, while Wolfe et al. (1995), on the basis of the LBQS DLA survey, find $\gamma = 1.15 \pm 0.55$, consistent with the absence of evolution.

This difference most probably arises in the value adopted for $(d\mathcal{N}/dz)_0$: RTB had fixed it at 0.015, as found by Rao (1994) in studying nearby galaxies, while Wolfe et al. had this parameter free, and found 0.055 ± 0.007. Indeed, these two determinations of γ would not be significantly modified if the value of $d\mathcal{N}/dz$ at $z \simeq 0.7$ as given in the RTB or LWT surveys were removed from the fit, as it is affected by large error bars. The best compromise to these conflicting results is to assume that rapid evolution occurs at $z < 1.7$ – where lensing is the most effective –, while a milder or no evolution takes place at higher-redshift.

3 Column density distribution function

In this section, we show how the column density distribution function can be evaluated, first without lensing, then by taking the by-pass effect and the amplification bias into account.

3.1 Without lensing effects

The damped Ly-α systems are especially interesting to study as they provide a direct estimate of the content of H I present in galaxies, or more generally, in collapsed objects. Indeed, following Lanzetta et al. (1991), the mean comoving density of gas, expressed in units of the critical density $\rho_{\rm crit} = (3H_0^2)/(8\pi G)$, located in DLAs at a redshift z is, in the absence of selection effects (lensing or dust, for example):

$$\Omega_{\rm HI}(z) = \frac{H_0}{c} \frac{m_{\rm H}}{\rho_{\rm crit}} \int_{N_{\rm DLA}}^{\infty} N\ f(N)\ dN, \tag{8}$$

where $m_{\rm H}$ is the mass of the hydrogen atom and $N_{\rm DLA}$ is the threshold column density to define a DLA. The column density distribution $f(N)$ is defined such that $f(N)\ dN\ dX$ represents the number of absorbers across the absorption distance interval dX with H I column density in the interval $[N,\ N+dN]$. The absorption distance is

$$dX = \frac{H_0}{c}\ (1+z)^3\ \frac{c\ dt}{dz}, \tag{9}$$

where, for a null cosmological constant,

$$\frac{c\ dt}{dz} = \frac{c}{H_0}\ \frac{1}{(1+z)^2}\ \frac{1}{\sqrt{1+2q_0 z}}. \tag{10}$$

As noticed by Tytler (1987), the observed slope of $f(N)$ is well represented by a power-law $f(N) \propto N^{-1.7}$ over the whole observed range of Ly-α line column densities. Because of this exponent value, the determination of the value of $\Omega_{\rm HI}$ is, a priori, mainly dependent on the largest column density observed in a given survey (i.e, the DLAs). However, this affirmation should not be taken too literally as explained in Sec. 4.

Observationally, $\Omega_{\rm HI}$ is easy to derive from a survey of DLA systems, as Eq. 8 writes:

$$\Omega_{\rm HI}^{\rm obs} = \frac{H_0}{c}\ \frac{m_{\rm H}}{\rho_{\rm crit}}\ \frac{\sum_{i=1}^{n_{\rm DLA}} N_{\rm i}}{\Delta X}, \tag{11}$$

where $n_{\rm DLA}$ is the number of DLAs detected in the survey, the $N_{\rm i}$ are their H I column density and ΔX is the survey total absorption distance path.

Following the simple models of column density distribution presented in Sec. 2, the systems with $N > N_{\rm HI}^{\rm max} \simeq 10^{21}\ {\rm cm}^{-2}$ only arise in inclined galaxies. Properly treating the inclination is thus important in order to evaluate the consequences of gravitational lensing on $f(N)$. The effects due to the possible presence of high column density clouds in the disk of galaxies is later discussed in Sec. 5.2.

Let R be the impact parameter of a LOS towards a background QSO, measured in the galaxy plane. Let $r = R/R_{\rm L}$, and $\theta = R/D_{\rm ol}$, where $D_{\rm ol}$ is the angular diameter distance between the observer and the galaxy. We first note that if the galaxy is inclined by an angle i, the observed H I column density is given by

$$N_{\rm HI}(r,i) = \frac{N_{\rm HI}(r,0)}{\cos i}, \tag{12}$$

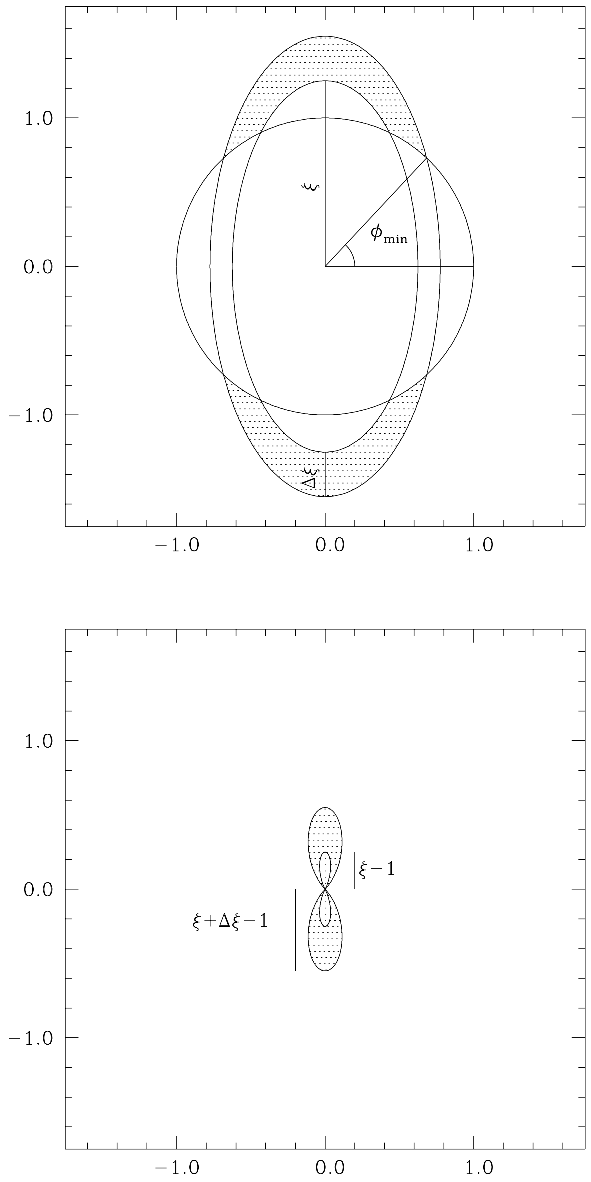

Fig. 2. Region that gives rise to an observed column density N in the range $[N_{\mathrm{face-on}}/\cos i, (N_{\mathrm{face-on}}+\Delta N_{\mathrm{face-on}})/\cos i]$ in Einstein radius units, assuming that $\xi > 1$ and $\xi \cos i < 1$: (a) in the image plane (up) and (b) in the source plane (down). ϕ_{min} is defined in the text. The figure corresponds to a galaxy disk inclined by $i = 60°$.

assuming that the thickness of the H I disk is very small compared to its diameter.

Similarly, we define Δr and $\Delta N(r, i)$ such that, in the linear approximation, $N(r+\Delta r, i) = N(r, i) + \Delta N(r, i)$ (note that ΔN may be positive or negative); in addition, $\Delta R = \Delta r\ R_{\mathrm{L}}$ and $\Delta\theta = \Delta R/D_{\mathrm{ol}}$. On the plane of the sky, the region that gives rise to a value of $N_{\rm HI}$ in the range $[N, N + \Delta N]$ is then given by an elliptical ring with variable width: the semi-major axes are given by r and $r + \Delta r$, and the semi-minor axes by $r \cos i$ and $(r + \Delta r) \cos i$, alike the elliptical ring represented in Fig. 2a in units that are defined below.

By definition, the distribution of column densities in the interval $[N, N+\Delta N]$ across the absorption distance interval $\Delta X = X(z_{\rm max}) - X(z_{\rm min})$ – corresponding to the redshift range $[z_{\rm min}, z_{\rm max}]$ – is:

$$f(N) = \frac{1}{\Delta X} < \left| \frac{\Delta P}{\Delta N} \right| >, \tag{13}$$

where ΔP represents the probability that the LOS crosses the elliptical ring defined by r, Δr and i. In the following, $P = P_{\rm GL}$ or $P_{\rm NL}$ as lensing is taken or not taken into account. The symbol $< \quad >$ represents the average over all inclinations. In the following, we shall drop the $|\ |$ symbol, so that ΔN represents its absolute value. For a constant value of ΔN, as used in observational works, one has

$$f(N) = \frac{1}{\Delta X} \frac{< \Delta P >}{\Delta N}. \tag{14}$$

The quantity $< \Delta P >$ is more precisely obtained by the following multiple integration:

$$< \Delta P > \quad = \int_{z_{\rm min}}^{z_{\rm max}} \int_{L_{\rm min}}^{L_{\rm max}} \frac{\int_{i_{\rm min}}^{\pi/2} \sin i \ dP}{\int_0^{\pi/2} \sin i \ di}, \tag{15}$$

where $i_{\rm min}$ takes into account the fact that high column density systems only arise in highly inclined disks:

$$\begin{aligned} i_{\rm min} &= 0 && \text{if } N \le N_{\rm HI}^{\rm max}, \\ &= \arccos\left(\tfrac{N_{\rm HI}^{\rm max}}{N}\right) && \text{if } N > N_{\rm HI}^{\rm max}. \end{aligned} \tag{16}$$

All the calculations that follow have been carried out with $L_{\rm min} = L_*/10$ and $L_{\rm max} = 10\ L_*$. The probability $dP(b_{\rm q}, z_{\rm q}; N, \Delta N, z, L, i)$ that a DLA has a column density in the range $[N, N + \Delta N]$, lies at a redshift in the range $[z, z + dz]$, arises in a galaxy with luminosity in the range $[L, L + dL]$ inclined by an angle in the range $[i, i + di]$ along the LOS, appears in the spectrum of a QSO whose redshift is $z_{\rm q}$ and magnitude $b_{\rm q}$, is:

$$dP(b_{\rm q}, z_{\rm q}; N, \Delta N, z, L, i) = \Phi(\frac{L}{L_*})\ (1+z)^{\gamma}\ \frac{c}{H_0}\ \Sigma_{\rm NL}\ F\ B\ \frac{dL}{L_*}\ dz\ di. \tag{17}$$

We have here assumed that $R_{\rm L}$ does not evolve with z. In other words, our model is still valid if the evolution indicated by the value $\gamma = 2.27$ found by RTB is only due to an evolution in the number density of galaxies. Here $\Sigma_{\rm NL}$ represents the cross-section in the absence of lensing and corresponds to the area of the whole elliptical ring (i.e. shaded and not-shaded areas) shown in Fig. 2a, and is given by:

$$\Sigma_{\rm NL} = 2\pi\ D_{\rm ol}^2\ \theta\ \Delta\theta\ \cos i, \quad \text{for } \Delta\theta \ll \theta. \tag{18}$$

In the absence of lensing, both B and F are set equal to 1 in Eq. 17, and ΔP is independent of $b_{\rm q}$, $z_{\rm q}$ and H_0. We shall now describe the two gravitational lensing effects which determine the new form of the expressions F and B in Eq. 17.

3.2 The by-pass effect

The lens equation can be written as

$$\theta = \theta_{\rm S} + \frac{D_{\rm ls}}{D_{\rm os}}\alpha \tag{19}$$

where $\theta_{\rm S}$ is the angular separation between the center of the lensing galaxy and the true QSO position and α is the angular value of the deflection of light (cf. Refsdal & Surdej 1994). For a SIS lens model,

$$\alpha = 4\pi\frac{\sigma^2}{c^2}, \tag{20}$$

and is thus independent of the impact parameter R (cf. Refsdal & Surdej 1994). As usual, $D_{\rm ls}$ and $D_{\rm os}$ are the angular-diameter distances between the lens and the source and the observer and the source, respectively.

Hence, this equation implies that the observed LOS towards a distant quasar must 'by-pass' the galaxy center, more precisely, the region inside the disk defined by the angular Einstein radius

$$\theta_{\rm E} = \frac{D_{\rm ls}}{D_{\rm os}}\ \alpha. \tag{21}$$

We also assume that any secondary lensed image, whenever present (i.e. in this model, if $\theta_{\rm S} < \theta_{\rm E}$) would be too weak to allow the detection of a DLA line in the integrated spectrum if it is not already present in the spectrum of the primary image. This effect must thus be properly taken into account when computing the cross-section $\Sigma_{\rm GL} = \Sigma_{\rm NL} F$ (cf. Fig. 2a).

Defining $\xi = \theta/\theta_{\rm E}$, we have to deal with 3 cases (assuming that $\Delta\xi = \Delta\theta/\theta_{\rm E}$ is small):

(i) $\xi < 1$: the whole elliptical ring lies within the Einstein one; no DLA can be produced in the corresponding elliptical ring: F and $\Sigma_{\rm GL}$ are set equal to 0;

(ii) $\xi > 1$ and $\xi \;\cos i < 1$: only part of the elliptical ring lies outside the Einstein radius, as shown by the shaded area in Fig. 2a, thus $\Sigma_{\rm GL} > 0$. The minimum angle that defines the 'allowed' region on the plane of the sky $\phi_{\rm min}$ is such that

$$\cos\phi_{\rm min} = \frac{\sqrt{(\xi+\Delta\xi)^2 - 1}}{\tan i}; \tag{22}$$

(iii) $\xi \;\cos i > 1$: the whole elliptical ring can give rise to DLAs and $\phi_{\rm min} = 0$.

Furthermore, this by-pass effect leads to a second consequence: the region *in the source plane* where the QSO must be located in order to produce a DLA in the considered elliptical ring is the shaded zone illustrated in Fig. 2b. In accordance with Eq. 19, its area $\Sigma_{\rm GL}$ can be much smaller than the corresponding shaded area *in the image plane* shown in Fig. 2a, even if $\xi \;\cos i > 1$. Indeed, using ζ to indicate that the integration is carried on over the source plane, we have

$$\Sigma_{\rm GL} = 4\; D_{\rm ol}^2\; \theta_{\rm E}^2 \int\limits_{\phi_{\rm min}}^{\pi/2} d\phi \int\limits_{\zeta_{\rm min}(i,\phi,\xi)}^{\zeta_{\rm max}(i,\phi,\xi,\Delta\xi)} \zeta\; d\zeta, \tag{23}$$

with

$$\zeta_{\rm min}(i,\phi,\xi) = \max\left(\frac{\xi}{\sqrt{1+\tan^2 i\;\; \cos^2\phi}}, 1\right) - 1, \tag{24}$$

$$\zeta_{\rm max}(i,\phi,\xi,\Delta\xi) = \frac{(\xi+\Delta\xi)}{\sqrt{1+\tan^2 i\;\; \cos^2\phi}} - 1. \tag{25}$$

Note that $\Sigma_{\rm NL}$ can be similarly written as (note the differences in the integration domains):

$$\Sigma_{\rm NL} = 4\; D_{\rm ol}^2\; \theta_{\rm E}^2 \int\limits_{0}^{\pi/2} d\phi \int\limits_{\xi_{\rm min}(i,\phi,\xi)}^{\xi_{\rm max}(i,\phi,\xi,\Delta\xi)} \xi'\; d\xi', \tag{26}$$

where

$$\xi_{\rm min}(i,\phi,\xi) = \frac{\xi}{\sqrt{1+\tan^2 i\ \cos^2\phi}}, \tag{27}$$

$$\xi_{\rm max}(i,\phi,\xi,\Delta\xi) = \frac{(\xi+\Delta\xi)}{\sqrt{1+\tan^2 i\ \cos^2\phi}}. \tag{28}$$

The by-pass effect thus decreases the effective cross-section by a factor $F(z_{\rm q},\xi,\Delta\xi,z,L,i)$:

$$\begin{aligned} F &= \tfrac{\Sigma_{\rm GL}}{\Sigma_{\rm NL}} \text{ if } \xi > 1, \text{ and} \\ &= 0, \quad \text{otherwise.} \end{aligned} \tag{29}$$

Fig. 3 illustrates the behaviour of F as a function of ξ for different values of i. We note that the by-pass effect is independent of H_0, and only weakly dependent on q_0, from the distances involved in Eq. 21 and thus also from $\phi_{\rm min}$.

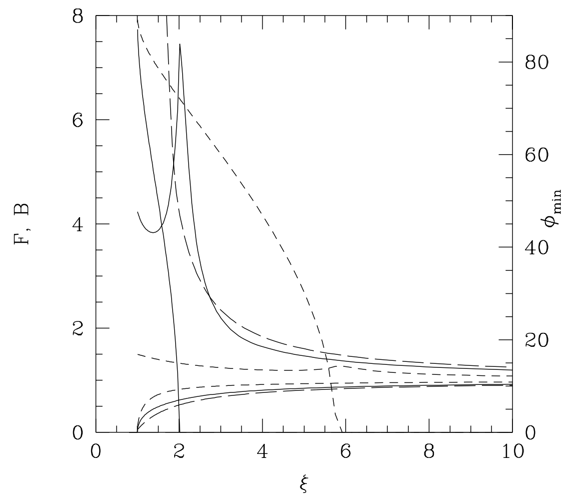

Fig. 3. Dependence of F (lower curves) and B(upper curves) on i, as a function of ξ. Solid: $i = 60^o$, short-dash: $i = 80^o$, long-dash: $i = 0^o$. The lines starting at $\xi = 2$ and $\xi = 6$ represent $\phi_{\rm min}$ for which the ordinate values are given on the right side ($\phi_{\rm min} = 0^o$ for $i = 0^o$). Computed for a L_* galaxy in front of a $z_{\rm q} = 2.5$, $b_{\rm q} = 16$ quasar; the ring was defined with $R = 1.5\ h^{-1}$ kpc, $\Delta R = 0.11\ h^{-1}$ kpc. Note that B reaches a maximum when $\phi_{\rm min}$ varies slowly with ξ.

3.3 The amplification bias

The amplification bias factor $B(b_{\mathrm{q}})$, as introduced by Gott & Gunn (1974; see also Fukugita & Turner 1991), accounts for the fraction of QSOs which appear brighter than a given apparent magnitude b_{q} due to GL. In statistical studies of multiply imaged quasars, $B(b_{\mathrm{q}})$ can be evaluated following the relation [2]

$$B(b_{\mathrm{q}}) = \int\limits_{A_{\min}}^{A_{\max}} \frac{N_{\mathrm{q}}(b_{\mathrm{q}} + 2.5 \log A)}{N_{\mathrm{q}}(b_{\mathrm{q}})} p(A) dA, \tag{31}$$

where $N_{\mathrm{q}}(b_{\mathrm{q}})$ is the intrinsic number counts of QSOs with magnitude b_{q} per solid angle and magnitude units. The function $p(A)$ represents the probability of obtaining an amplification A for the considered lens model. The integration limits are fixed by the physical problem under study. For example, they can be set by the constraint of having multiple images, which in the case of the SIS lens model correspond to $A_{\mathrm{min}} = 2$ and $A_{\mathrm{max}} = \infty$.

However, a more general expression is needed in order to evaluate $B(b_{\mathrm{q}})$: in our case, the expression must be evaluated by taking into account geometrical considerations. The value of A obviously depends on the position(s) of the image(s) in the image plane. If $\mathcal{S}$ is the domain in the source plane corresponding to the one of interest in the image plane, and is mapped by the polar coordinates θ_{S} and ϕ, we thus have:

$$B(b_{\mathrm{q}}, \mathcal{S}) = \frac{\iint_{\mathcal{S}} N_{\mathrm{q}}(b_{\mathrm{q}} + 2.5 \log A(\theta_{\mathrm{S}}, \phi))\ \theta_{\mathrm{S}}\ d\theta_{\mathrm{S}}\ d\phi}{N_{\mathrm{q}}(b_{\mathrm{q}})\ \iint_{\mathcal{S}} \theta_{\mathrm{S}}\ d\theta_{\mathrm{S}}\ d\phi}. \tag{32}$$

It should be noted that both the numerator and the denominator correspond to an integral evaluated over the *same* domain in the *source* plane. Thus, a correct comparison between the lens and the no-lens cases must always take the amplification bias and by-pass effects simultaneously into account (i.e. also for the statistics of multiple images).

---

[2] Because the number counts of quasars are usually given as a function of their blue magnitude b_{j} but catalogs only list V magnitudes, or the magnitude (B or m_{pg}) if present in the original publication, we can apply a conversion using the following color terms, following Véron-Cetty and Véron (1991):

$$\begin{aligned} b_{\mathrm{j}} - V &= 0.12 + 0.787\ (z_{\mathrm{q}} - 0.5),\ \text{if}\ z_{\mathrm{q}} < 0.9; \\ &= 0.40 - 0.231\ (z_{\mathrm{q}} - 0.9),\ \text{if}\ 0.9 \leq z_{\mathrm{q}} \leq 2.2; \\ &= 0.10 + 0.708\ (z_{\mathrm{q}} - 2.2),\ \text{if}\ z_{\mathrm{q}} > 2.2. \end{aligned} \tag{30}$$

In the case of an elliptical ring, the amplification bias is given by the following relation, where we have taken advantage of the axis-symmetry of the SIS lens, and assumed that any secondary lensed image (whenever present) would be too weak to allow detection of a DLA line in the integrated spectrum if there is no DLA in the spectrum of the primary one:

$$B(b_{\rm q};\xi,\Delta\xi,i) = 4\;\frac{R_{\rm E}^2}{\Sigma_{\rm GL}}\int\limits_{\phi_{\rm min}}^{\pi/2} d\phi \int\limits_{\zeta_{\rm min}(i,\phi,\xi)}^{\zeta_{\rm max}(i,\phi,\xi,\Delta\xi)} \frac{N_{\rm Q}(b_{\rm q}+2.5\log A(\zeta))}{N_{\rm Q}(b_{\rm q})}\;\zeta\;d\zeta. \tag{33}$$

Expressing ζ in terms of A leads to the more usual form:

$$B(b_{\rm q};\xi,\Delta\xi,i) = 4\int\limits_{\phi_{\rm min}}^{\pi/2} d\phi \int\limits_{A_{\rm min}(i,\phi,\xi,\Delta\xi)}^{A_{\rm max}(i,\phi,\xi)} \frac{N_{\rm Q}(b_{\rm q}+2.5\log A)}{N_{\rm Q}(b_{\rm q})}\;p_{\rm R}(A)\;dA, \tag{34}$$

where the amplification probability for an elliptical ring $p_{\rm R}(A)$ is given by:

– $1 < A \leq 2$:

$$p_{\rm R}(A)dA = \frac{R_{\rm E}^2}{2\;\Sigma_{\rm GL}}\;\frac{2\;dA}{(A-1)^3}, \tag{35}$$

– $A > 2$:

$$p_{\rm R}(A)dA = \frac{R_{\rm E}^2}{2\;\Sigma_{\rm GL}}\;\frac{8\;dA}{A^3}. \tag{36}$$

Note that $p_{\rm R}(A)$ is discontinuous at $A = 2$ with the appearance of a secondary lensed image, but that B does not present any discontinuity. The integration limits are given by:

– if $\zeta_{\rm min}(i,\phi,\xi) < 1$ and $\zeta_{\rm max}(i,\phi,\xi,\Delta\xi) < 1$:

$$\begin{aligned} A_{\rm min}(i,\phi,\xi,\Delta\xi) &= \frac{2}{\zeta_{\rm max}(i,\phi,\xi,\Delta\xi)}, \\ A_{\rm max}(i,\phi,\xi) &= \frac{2}{\zeta_{\rm min}(i,\phi,\xi)}; \end{aligned} \tag{37}$$

– if $\zeta_{\rm min}(i,\phi,\xi) < 1$ and $\zeta_{\rm max}(i,\phi,\xi,\Delta\xi) > 1$:

$$\begin{aligned} A_{\rm min}(i,\phi,\xi,\Delta\xi) &= 1+\frac{1}{\zeta_{\rm max}(i,\phi,\xi,\Delta\xi)}, \\ A_{\rm max}(i,\phi,\xi) &= \frac{2}{\zeta_{\rm min}(i,\phi,\xi)}; \end{aligned} \tag{38}$$

– if $\zeta_{\rm min}(i,\phi,\xi) > 1$ and $\zeta_{\rm max}(i,\phi,\xi,\Delta\xi) > 1$:

$$
\begin{aligned}
A_{\rm min}(i,\phi,\xi,\Delta\xi) &= 1 + \frac{1}{\zeta_{\rm max}(i,\phi,\xi,\Delta\xi)}, \\
A_{\rm max}(i,\phi,\xi) &= 1 + \frac{1}{\zeta_{\rm min}(i,\phi,\xi)}.
\end{aligned}
\tag{39}
$$

The observed quasar number counts can be modeled by a broken power-law, as given by Hartwick & Schade (1990):

$$
N_{\rm Q} \propto 10^{c(b_{\rm q})\ (b_{\rm q}-19.15)}, \tag{40}
$$

with

$$
\begin{aligned}
c(b_{\rm q}) &= 0.86, \ \text{if } b_{\rm q} < 19.15, \\
c(b_{\rm q}) &= 0.28, \ \text{if } b_{\rm q} > 19.15.
\end{aligned}
\tag{41}
$$

If we approximate $c(b_{\rm q})$ by the values 0.9 and 0.3, respectively, – well within the error bars –, Eq. 34 can be expressed analytically. The important point here is that the amplification bias strongly depends on the steepness of the slope of $N_{\rm Q}$: it is very efficient for QSO magnitude on the steep part of $N_{\rm Q}$ and of little importance for $b_{\rm q} > 19.15$. The behaviour of B is presented in Fig. 3.

We note that, here also, the amplification bias is independent of H_0, but slightly depends on q_0, through $\phi_{\rm min}$, and thus $A_{\rm min}$ and $A_{\rm max}$.

Finally, the calculation of $\Delta P_{\rm GL}$ is obtained by inserting in Eq. 17 the expressions of F and B given in Eq. 29 and Eq. 34.

4 Results

In this section, we shall discuss the effects of GL on the column density distribution $f(N)$, on the value of $\Omega_{\rm HI}$, on the luminosity distribution of the galaxies responsible for the DLAs and on the possibility to detect them in a given survey.

We have evaluated $f(N)$ numerically assuming the two models of column density profiles described in Sec. 2.

4.1 Effects on $f(N)$

Let us first recall that, in the absence of lensing, the curve $f(N)$ can be divided in two parts in the range of interest (cf. Fig. 4; see also Fig. 7 of Rao & Briggs 1993). Indeed, a useful, empirical representation is[3] :

$$f(N) \propto O_{\mathrm{f}}(N) \left(f_1(N)\ \chi_{]N_{\mathrm{min}}, N_{\mathrm{HI}}^{\mathrm{max}}]} \ + \left(\frac{N_{\mathrm{HI}}^{\mathrm{max}}}{N}\right)^3 \ \chi_{]N_{\mathrm{HI}}^{\mathrm{max}}, \infty[} \right), \tag{42}$$

where $O_{\mathrm{f}}(N) = f_{\mathrm{GL}}(N)/f_{\mathrm{NL}}(N)$ takes into account the lensing effects, and where χ stands for the Heaviside function. The value $N_{\mathrm{HI}}^{\mathrm{max}}$ appears naturally in this curve as the abscissa of the inflexion point. The column density N_{min} represents the minimum value for which Eq. 42 is valid; in any case, $N_{\mathrm{min}} < N_{\mathrm{DLA}}$: for example, it may be the abscissa of the inflexion point between the low-column density Ly-α systems and the high-column density ones which include the DLAs, in which case $N_{\mathrm{min}} \simeq 10^{19}$ cm^{-2}. On the other hand, the function $f_1(N)$ depends on the column density profile. For the E+GH model, a power-law provides a good empirical approximation in the range of interest:

$$f_1(N) = \left(\frac{N_{\mathrm{HI}}^{\mathrm{max}}}{N}\right)^{1.25}, \tag{43}$$

while an exact representation can be derived for the E model[4] :

$$f_1(N) = \frac{N_{\mathrm{HI}}^{\mathrm{max}}}{N} \left[2\ \ln\left(\frac{N_{\mathrm{HI}}^{\mathrm{max}}}{N}\right) + 1 \right]. \tag{44}$$

If we compare the curve $f(N)$ that we obtain for the E+GH model with the one presented in Fig. 7 of Rao & Briggs (1993), then we note the following differences: 1) if we associate the abscissa of the inflexion point in their curve $f(N)$ with $N_{\mathrm{HI}}^{\mathrm{max}}$, then their value of $N_{\mathrm{HI}}^{\mathrm{max}}$ is larger than the one we have adopted ($\simeq 10^{21}$ cm^{-2} compared to our $10^{20.8}$ cm^{-2}); 2) we obtain a steeper $f_1(N)$, as their curve in the $N < N_{\mathrm{HI}}^{\mathrm{max}}$ part is best represented by the power-law $f_1(N) = \left(\frac{N_{\mathrm{HI}}^{\mathrm{max}}}{N}\right)^{1.1}$; as a consequence, we also remark that our curves $f(N)$

[3] Milgrom (1988) discusses such power laws, and, in particular, notes that the N^{-3} part of the curve arises independently of the surface-density profile of the disk, provided it decreases with r.

[4] In fact, for the E model in the absence of lensing, $f(N)$ can be derived analytically over the whole range of interest as

$$f(N) \propto \left(\frac{N_{\mathrm{HI}}^{\mathrm{max}}}{N} \left[2\ \ln\left(\frac{N_{\mathrm{HI}}^{\mathrm{max}}}{N}\right) + 1 \right] \chi_{]N_{\mathrm{min}}, N_{\mathrm{HI}}^{\mathrm{max}}]} + \left(\frac{N_{\mathrm{HI}}^{\mathrm{max}}}{N}\right)^3 \ \chi_{]N_{\mathrm{HI}}^{\mathrm{max}}, \infty[} \right).$$

evaluated at $\log N = 19$ are a factor $\simeq 3$ larger. Although this fact may be important in understanding the evolution with z of the product of the cross-section by the number density of DLAs, we leave this point open for a more detailed analysis [5]

In addition, as seen in Fig. 4, our curve $f(N)$ for the E+GH model shows a bump at $N = N_{\rm HI}^{\rm max}$ (even in the absence of lensing effects) due to the fact that $N_{\rm HI}(r)$ presents a maximum. This bump does not appear in Fig. 7 of Rao & Briggs; instead, the $N < N_{\rm HI}^{\rm max}$ part in their figure presents a small curvature, probably due to the fact that the 27 galaxies used for its construction have different values of $r_{\rm max}$ and $N_{\rm HI}^{\rm max}$.

From now on, we shall only derive ratios between quantities calculated by taking lensing into account to the ones computed without lensing; as a consequence, it will appear that the differences between our estimates of $f(N)$ and the one obtained by Rao & Briggs are not important for our purpose, except for the value of $N_{\rm HI}^{\rm max}$.

Indeed, gravitational lensing does not strongly affect the slope of the $f(N)$ curve. Instead, GL produces a small bump close to $N_{\rm HI}^{\rm max}$, and mainly a shift of the N^{-3} part towards larger values of N (cf. Fig. 4). Indeed, as seen in Fig. 5 for the extreme case of lensing scenario, GL may introduce an overdensity of up to a factor $\simeq 4$ in the case of the E+GH model, and $\simeq 3$ in the case of the E model. Hence, GL mainly affects the large N DLAs, which are only produced in highly inclined galaxies. The main reason for the difference between the two models lies in the distinct slopes of the $N_{\rm HI}(r)$ relations: the GL effects are stronger if $N_{\rm HI}(r)$ decreases quickly with r; on the other hand, the presence of a Gaussian hole in the $N_{\rm HI}(r)$ relation results in slightly displacing the bump close to $N_{\rm HI}^{\rm max}$ towards lower values of N.

4.2 Number density of DLA systems

The number density $d\mathcal{N}/dz$ of DLA systems per unit redshift is given by integrating $f(N)$ over the range $N > N_{\rm DLA} = 2\ 10^{20}$ cm^{-2}. The numerically calculated ratio $(\frac{d\mathcal{N}}{dz})_{\rm GL}/(\frac{d\mathcal{N}}{dz})_{\rm NL}$, which describes the expected overdensity of DLA systems due to lensing, is represented in Fig. 6. It was computed for

[5] In this respect, we note that Eq. 6 of Wolfe et al. (1986) under-estimates the value of the average cross-section of an H I disk. Indeed, their formula does not take into account the contribution to the cross-section arising from lines-of-sight intercepting sufficiently inclined galactic disks outside their H I radius. In other words, Eq. 6 of Wolfe et al. assumes that galactic disks present a sharp edge located at $r = r_{\rm DLA}$ outside which H I is absent. A correct formula depends on the H I density profile of the disk. This error also affects our Eq. 6 and leads to a decrease of our $f(N)$.

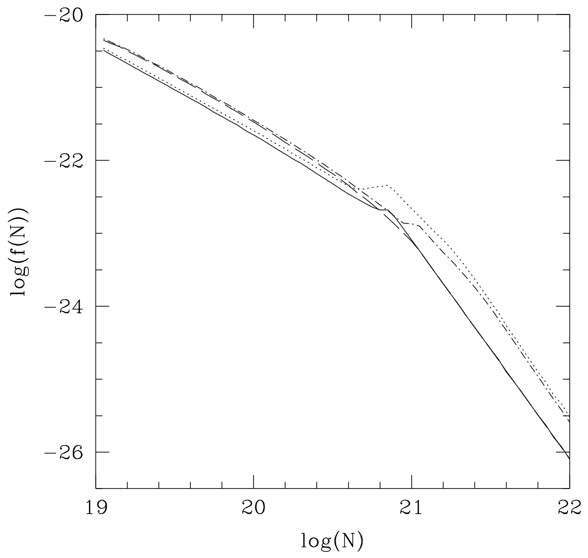

Fig. 4. Column density distribution $f(N)$ for $z = 0.5$ DLAs in front of a $z_q = 2.5$, $b_q = 16$ QSO. Without lensing (solid) and with lensing effects for the E+GH model (dot). Without lensing (long dash) and with lensing effects for the E model (dot-short dash). Curves computed in redshift intervals of 0.01, and $q_0 = 1/2$.

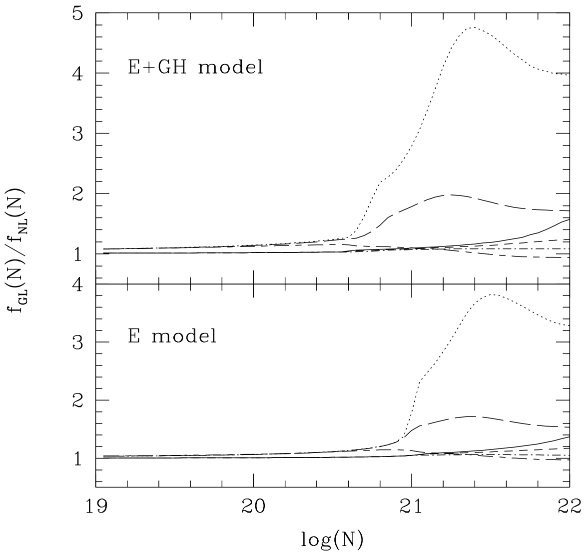

Fig. 5. For both the E+GH (top) and E (bottom) models, we have illustrated the ratio $f_{\rm GL}/f_{\rm NL}$ for a $z_q = 2.5$ QSO and: A) for $z = 0.5$ DLAs, and $b_q = 16$ (dot), $b_q = 18$ (long dash), $b_q = 20$ (short dash - long dash); B) for $z = 2.0$ DLAs, and $b_q = 16$ (solid), $b_q = 18$ (short dash), $b_q = 20$ (dot - short dash). Curves computed in redshift intervals of 0.01.

the E and E+GH models, for both a $z_q = 2.5$ and a $z_q = 1.0$ QSO, and for different values of b_q. In the computations, a step $dz = 0.05$ was used. One sees that the number density of DLAs may be overestimated by up to $\simeq 90\%$

in front of very bright ($b_q \simeq 16$), high-z ($z_q > 1$) QSOs, for the E+GH model; this value decreases to $\simeq 35$ % for the E model.

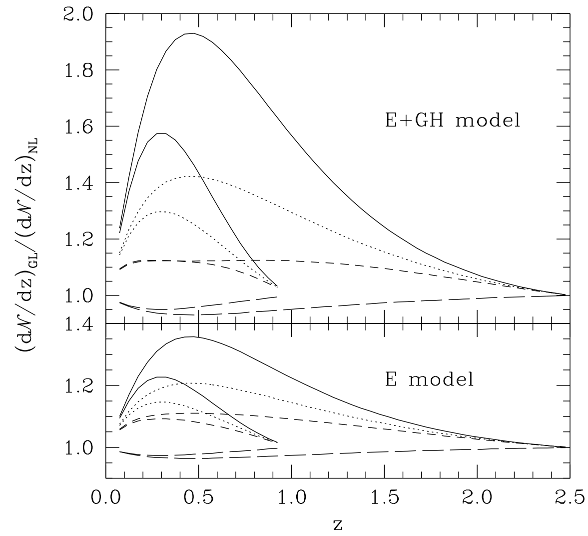

Fig. 6. For both the E+GH (top) and E (bottom) models, we have illustrated the ratio $(d\mathcal{N}/dz)_{\rm GL}/(d\mathcal{N}/dz)_{\rm NL}$ for DLAs in front of $z_q = 1.0$ and $z_q = 2.5$ QSOs. The curves correspond to $b_q = 16$ (solid), $b_q = 18$ (dot), $b_q = 19$ (short dash), $b_q = 20$ (long dash). Curves computed in redshift intervals of 0.05, and for $q_0 = 1/2$.

It is also clear that for $b_q > 19.15$, the by-pass effect dominates the amplification bias.

In Fig. 7, we show how the number density of DLAs in the range $0.3 < z < 0.7$ ($1.7 < z < 2.0$) changes as the redshifts of the quasars increase, for different values of their magnitudes.

4.3 Effects on $\Omega_{\rm HI}$

The determination of $\Omega_{\rm HI}$ at high-z is not significantly affected by gravitational lensing effects. Indeed, as seen in Fig. 8, $\Omega_{\rm HI,GL}/\Omega_{\rm HI,NL}$ is ≈ 1.10 for $z = 2$ DLAs in front of $z_q = 2.5, b_q > 16$ QSOs. Only in extreme lensing cases can the over-estimate reach important factors: $\simeq 170\%$ for the E+GH model ($\simeq 90\%$ for the E model) for $z = 0.5$ DLAs in front of $z_q = 2.5$, $b_q = 16$ QSOs, but already decreases to 60% (35%) for $b_q = 18$ QSOs.

It is somewhat surprising that the determination of $\Omega_{\rm HI}$ is only relatively mildly affected by the strong lensing effect on the largest column density systems: it is usually thought that they mostly determine its value because of the $N^{-1.7}$ overall dependence of $f(N)$. However, the explanation is clear from

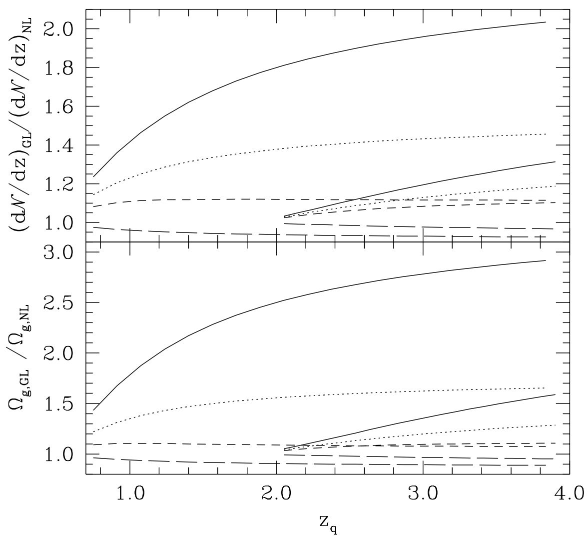

Fig. 7. Influence of gravitational lensing effects as a function of z_q on the determination of $d\mathcal{N}/dz$(top) and Ω_{HI} (bottom) for DLAs in the redshift range $0.3 < z < 0.7$ and $1.7 < z < 2.0$, for $b_q = 16$ (solid), 18 (dot), 19 (short-dash) and 20 (long-dash). The E+GH model was used to derive these curves.

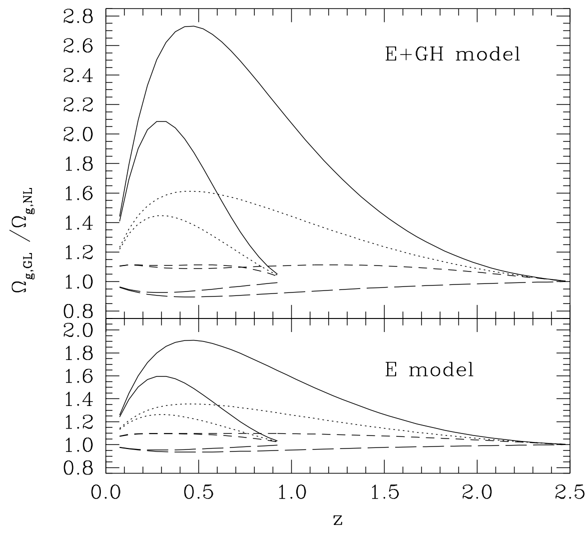

Fig. 8. Influence of lensing effects on the determination of Ω_{HI} in front of $z_q = 1.0$ and $z_q = 2.5$ QSOs, for both the E+GH (top) and E (bottom) models. The curves correspond to $b_q = 16$ (solid), $b_q = 18$ (dot), $b_q = 19$ (short dash) and $b_q = 20$ (long dash). Curves computed in redshift intervals of 0.05, and for $q_0 = 1/2$.

Eq. 42: in fact, the largest column density system arise in the N^{-3} part of the curve $f(N)$.

In the absence of lensing $O_f = 1$; hence, for the E+GH model (E model), only

$\simeq 57\%$ (35%) of $\Omega_{\rm HI}$ depends on the column density systems with $N > N_{\rm HI}^{\rm max}$; the other $\simeq 43\%$ (65%) arises from N in the domain $[N_{\rm DLA}, N_{\rm HI}^{\rm max}]$ [6].

Fig. 7 also shows how the determination of $\Omega_{\rm HI}$ based on the observation of DLAs in the range $0.3 < z < 0.7$ ($1.7 < z < 2.0$) changes as the quasar redshift increases, for different values of their magnitudes.

4.4 Effects on the luminosity distribution of the DLA galaxies

Following Eqs. 1, 2, 20 and 21, it is straightforward to establish that:

$$\frac{1}{\xi} \propto \left(\frac{L}{L_*}\right)^{2/\alpha_{\rm TF}-\alpha_{\rm H}}, \tag{45}$$

where $2/\alpha_{\rm TF} - \alpha_{\rm H} = 0.35$ for the values adopted above (i.e. $\alpha_{\rm TF} = 2.6$ and $\alpha_{\rm H} = 5/12$).

The quantity $\int_{N_{\rm inf}}^{\infty} f_{\rm GL}(N)dN / \int_{N_{\rm inf}}^{\infty} f_{\rm NL}(N)dN$ as a function of L is represented in Fig. 9, obtained for $\log N_{\rm inf} = 20.3$ and 21, and for $\alpha_{\rm TF} = 2.6$ and 4. The model E+GH was used for $b_{\rm q} = 16$, $z_{\rm q} = 2.5$ QSOs and $z = 0.5$ DLAs. Hence, a strong overdensity of bright galaxies causing the DLAs is expected for $\log N_{\rm HI} \gtrsim 21$, but its importance depends on the values of $\alpha_{\rm TF}$ and $\alpha_{\rm H}$.

In particular, we note that for $2/\alpha_{\rm TF} < \alpha_{\rm H}$, the overdensity affects the faint galaxies, while the bright ones are under-represented relatively to the density of L_* galaxies (dotted line in Fig. 9)! A significant overdensity is still expected at rather large redshift for $\alpha_{\rm TF} = 2.6$ and $\alpha_{\rm H} = 5/12$: bright galaxies ($L > L_*$) at $z \simeq 2$ should present an overdensity $> 12\%$ (relative to the unlensed case) in front of $b_{\rm q} = 16$, $z_{\rm q} = 2.5$ QSOs, and 8% for $b_{\rm q} = 18$, $z_{\rm q} = 2.5$ QSOs.

4.5 Dependence on H_0 and q_0

As seen above, the lensing effects do not depend on the Hubble parameter. They only weakly depend on q_0: we find that for $z \sim 0.5$ DLAs in front of $b_{\rm q} = 16$, $z_{\rm q} = 2.5$ QSOs, there is only a 5% difference in the estimate of $\Omega_{\rm HI}$ between $q_0 = 1/2$ and $q_0 = 0.01$.

[6] Similarly, in absence of lensing, the value of $\Omega_{\rm HI}$ estimated in the range $N > N_{\rm DLA} = 2\ 10^{20}$ cm^{-2} – as in Eq. 8 – is only $\simeq 80$ % (70%) of the one estimated in the range $N > 10^{19}$ cm^{-2} for the E+GH model (E model).

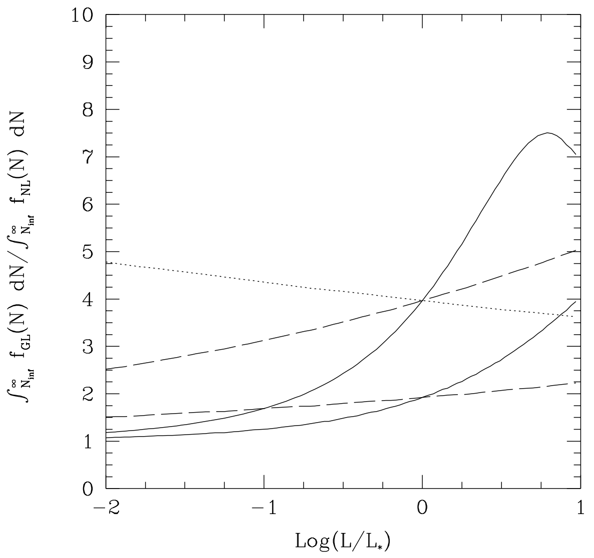

Fig. 9. Influence of lensing on the number of DLAs with $N_{\rm HI}$ larger than $N_{\rm inf}$, as a function of the luminosity of the galaxy responsible for the DLA. Solid: for $\alpha_{\rm TF} = 2.6$; dash: $\alpha_{\rm TF} = 4$; in both cases $\alpha_{\rm H} = 5/12$. For each of the two cases, the lower curve corresponds to $\log N_{\rm inf} = 20.3$ and the upper one to $\log N_{\rm inf} = 21.0$. The dotted line has been obtained with the parameters $\alpha_{\rm TF} = 2.6$, $\alpha_{\rm H} = 4/5$ and $\log N_{\rm inf} = 21.0$. The different curves were obtained for the E+GH model and correspond to $b_{\rm q} = 16$, $z_{\rm q} = 2.5$ QSOs and $z = 0.5$ DLAs.

4.6 A new lensing effect

As noted several times, the largest $N_{\rm HI}$ systems only arise in highly inclined galaxies, assuming the absence of any absorbing dense H I cloud. The largest column density systems (even in the no-lens case) thus tend to be located close to the line which is the intersection between the galaxy plane and the plane of the sky. By excluding any possibility of DLAs within the Einstein radius (except for the secondary lensed image of a multiply imaged QSO), GL further re-enforces this effect.

An interesting consequence is to offer the possibility to measure one point of the rotation curve of the galaxy giving rise to the high $N_{\rm HI}$ DLA, and thus to obtain a rough estimate of its mass. Indeed, a high-z galaxy probably has a too low surface brightness to enable us to derive its morphology and inclination –especially in the glow of the QSO–, but provided its spectrum presents emission lines, a precise value of its redshift can be derived. Comparison with the DLA redshift thus leads to the possibility of obtaining a lower value for its rotation velocity. Furthermore, if the impact parameter can be precisely determined from observations, an upper limit to the galaxy rotation velocity can be obtained from the absence of a secondary lensed image.

However, in practice, this effect is not likely to be important, since the Einstein radius is usually of the order of $\leq 1\ h^{-1}$ kpc.

4.7 Critics of the Bartelmann & Loeb study

Figure 4 shows that $f(N)$ only presents a small bump close to $N = N_{\rm HI}^{\rm max}$; more importantly, this curve does not present any sharp drop, very much in contrast to the results obtained by Bartelmann & Loeb (1996). It is easy to understand why this cannot be the case.

Indeed, Bartelmann & Loeb (1996) first compute the cross-section $\sigma(> N)$ to have a DLA with a column density larger than N, by taking into account the inclinations and the luminosities of galaxies, but no lensing effects yet.

They then introduce a quantity $r(> N) = \sqrt{\sigma(> N)/\pi}$, which represents the maximal value of the impact parameter that leads to a column density $> N$. In this way, they build a model of galaxy, *seen face-on*, which, from the point-of-view of DLA absorption is the proper average of luminosity and inclination characteristics.

The by-pass effects and amplification bias are then considered: all DLAs with $r(> N)$ smaller than the Einstein radius cannot be observed, which eliminate the largest N systems; the ones for which $r(> N)$ is just larger than the Einstein radius are preferentially selected in magnitude-limited samples of QSOs, so that their curve $f(N)$ presents a bump.

However, in such a treatment, they attribute a quality of (disk-like) shape to their cross-section. It is clear from Fig. 2 that this is not the case. The very high N systems always appear in highly inclined galaxies; they arise in elliptical rings for which a large fraction may lie outside the Einstein radius. As a consequence, the cross-section for these systems cannot be set equal to zero and the sharp drop seen in the $f(N)$ curves of Bartelmann & Loeb cannot be real.

Another way of interpreting their error is to realize that they did not compute the amplification bias at the same time as the effective geometrical cross-section, but only after averaging over all inclinations. However, these two calculations cannot be separated (cf. Section 3.3).

5 Caveats

The gravitational lensing situation that we have previously described contains a number of simplifications that we shall briefly summarize here.

5.1 Model of spiral galaxies

First, it is very likely that the exponents for the Tully-Fisher and Holmberg relations, or other quantities like σ_* or R_* do not have necessarily the same values at moderate or large redshifts, for example due to galaxy evolution. A significant increase in $R(L)$ would most probably have the largest effects on the estimates below, as the amplification bias is (coarsely) inversely proportional to the cross-section of the DLAs.

The basic assumption that DLAs arise in disks has received some confirmation from detailed analysis of the shape of line profiles in some DLAs (Wolfe et al. 1994, Prochaska & Wolfe 1996). Observations of DLAs along two close lines-of-sight, as provided by multiply imaged QSOs (Smette et al. 1995, 1996) or in front of extended radio-sources (Smith, Junkkarinen & Burbidge 1977, Briggs et al. 1989, Foltz, Chaffee & Wolfe 1988) are consistent with the hypothesis that they arise in disks of radius $\sim R_*$. The observed slope of $f(N)$ at large $N_{\rm HI}$ values is unfortunately badly constrained due to the small numbers of such systems observed so far. Its determination does not strongly depend on the exact distribution of $N_{\rm HI}(r)$ and would thus allow to confirm if the DLAs indeed arise in flattened or spherical objects (Milgrom 1988).

On the other hand, the hypothesis that H I disks have a negligible thickness probably breaks down for the $\log(N_{\rm HI}) = 22$ systems as they can only arise in galaxies inclined by more than 80^o in our model.

5.2 Column density profile

Second, there is no clue as to whether the actual column density distribution even in $z \sim 0.5$ galaxies do indeed follow one of the models discussed above. Even if it did, such models have been obtained from observations of 21 cm hydrogen in emission at relatively low spatial resolution, which smoothes out signal arising in regions of lower or higher column density relative to the average. On the contrary, lines-of-sight towards QSOs reveal column densities determined in very narrow beams: it is not *a priori* excluded that the spectra of some QSOs, although located behind the disks of spiral galaxies, do not show any high column density hydrogen line.

Similarly, high-column density DLAs may very well be produced in dense globules of gas, although the galaxy is seen nearly face-on and the impact parameter is rather large. Globally, such effects induce noise in the column density distribution, with the consequence that a large set of data is required in order to prove that gravitational lensing effects do indeed affect DLA surveys.

5.3 Lensing model

Third, the validity of the SIS model to describe lensing effects due to spiral galaxies may be affected if dark matter halos are flattened, as indicated by recent observations (cf. Sackett 1996), although quantifying the amount of ellipticity appears difficult. Similarly, the number of 5-image lens systems to the one of 3-image systems is much higher than expected in the Jodrell/VLA Astrometric Survey (JVAS), even taking different biases into account: King et al. (1996) advocates that a possible solution to this problem may be that some lenses are much more elliptical than previously thought; however, a definite conclusion on this point must await a better knowledge of the number counts for the very faint radio-sources in order to properly estimate the amplification bias.

Another problem with the SIS model arises as the presence of nearby galaxies or even large-scale structure can produce external asymmetric shear of the same order as the lens itself (Bar-Kana 1996), leading to a quadrupole lens. The 5 image configuration which results leads more easily to larger amplifications than possible with a SIS lens.

5.4 Amplification bias

Fourth, the amplification bias depends strongly on the *shape* of the number counts $N_{\rm q}(b_{\rm q})$ of quasars. The single power law advocated by Hawkins & Véron (1995) would produce mathematical problems, as some of the terms used to compute Eq. 34 would lead to infinities.

If the slope of the bright end (cf. Eq. 41) is steeper, the amplification bias can be much stronger. A break occurring at magnitude larger than 19.15 would more strongly affect the lensing effects on existing surveys described below. Statistics of multiply imaged quasars allow to constrain independently these parameters (cf Surdej et al. 1993; Claeskens, Jaunsen & Surdej 1996), but possible ranges remain large.

A radio search for DLAs (using the 21 cm line) in front of radio-selected quasars will also be subjected to the same effects as described here; however, the quasar number counts in radio must then be used. The estimate of lensing effects on a survey of DLAs in front of QSOs based on *both* optical and radio luminosities must take the double amplification bias into account (Borgeest, Linde & Refsdal 1991).

5.5 Unicity of the lens

Fifth, the considered lensing configuration (only at most one galaxy susceptible to produce a DLA lies along the LOS towards the QSO) is a huge simplification. It may well be that other (for example, elliptical) galaxies are closer to the LOS towards the QSO than the one producing the DLA; in this case, the QSO may appear brighter because of GL amplification, decreasing the importance of the amplification bias due to spiral galaxies. Preliminary calculations however indicate that elliptical galaxies are too rare for such an effect to be important.

Another possible situation occurs if a cluster of galaxies lies along the LOS, containing or not the galaxies responsible for the DLAs. Such a situation can also boost the QSO magnitude, and thus further increase the amplification bias.

Finally, micro-lensing by stars within spiral galaxies may also contribute to the amplification bias. Since the surface density of stars in a spiral galaxy and the H I column density are well correlated, amplification bias due to microlensing may turn out to be important.

5.6 Dust

Sixth, the presence of dust may significantly modify the results that we have presented. Indeed, corrections to the observed $f(N)$ at $z \sim 0.5$ – and thus $d\mathcal{N}/dz$ and $\Omega_{\rm HI}$ – because of gravitational lensing have the same order of magnitude, but in the opposite direction, as the estimates of the influence of dust extinction by Fall & Pei (1993, see also Pei & Fall 1995). However, it would be a mistake to conclude that the two effects compensate each other.

Indeed, the consequences of including both gravitational lensing effects and the ones due to extinction by dust are not obvious: (i) combination of the by-pass effect with the effect of dust will strongly depend on the distribution of dust within the galaxies: if dust is preferably concentrated centrally, the by-pass effect may just eliminate all dust effects; this will not be the case if, on the other hand, and much more realistically, the dust is uniformly distributed. (ii) The combination of the amplification bias with the extinction by dust leads to a counter-intuitive effect: indeed, extinction increases the apparent magnitude b_q of a quasar which presents a DLA in its spectrum; consequently, the estimate of the amplification bias for such QSOs will be underestimated since it strongly depends on (small values of) b_q, leading to underestimate the lensing effects.

However, this argument holds only as long as the QSO number counts relation is not affected by extinction: too large an extinction by dust leads to exclude background quasars from samples suitable for spectroscopy. A thorough examination of the combination of the effects of extinction by dust, and of macro- and micro-gravitational lensing are thus necessary before reaching any definite conclusion, and shall be investigated in a subsequent paper.

6 Observational aspects and statistical tests

We present here numerical determinations of $O_{d\mathcal{N}/dz} = (d\mathcal{N}_\mathrm{GL}/dz)/(d\mathcal{N}_\mathrm{NL}/dz)$ and $O_{\Omega_\mathrm{HI}} = \Omega_\mathrm{HI,GL}/\Omega_\mathrm{HI,NL}$ based on the E and E+GH models for the existing DLA surveys. We then discuss statistical tests to detect observationally the influence of lensing in a given survey.

We have considered (i) the IUE survey by Lanzetta et al. (1995, LWT), (ii) the high-z survey by Lanzetta et al. (1991) which includes the Lick survey initiated by Wolfe et al. (1986), and (iii) the LBQS survey by Wolfe et al (1995). We also study (iv) the RTB survey which restricts the search for DLAs to known Mg II systems, and for which the determination of the N_HI of the DLA candidates is not yet completed.

6.1 Estimates of lensing effects in existing surveys

The over-densities $O_{d\mathcal{N}/dz}$ and O_{Ω_HI} for each of these surveys are presented in Table 1 (the low and high IUE domains are defined below). They were obtained by first computing $f_\mathrm{GL}(N)$ and $f_\mathrm{NL}(N)$ from Eq. 13:

$$f(N) = \frac{\sum_{i=1}^{n_\mathrm{QSO}} < \left|\frac{\Delta P_i}{\Delta N}\right| >}{\sum_{i=1}^{n_\mathrm{QSO}} \left(X(z_{i,\max}) - X(z_{i,\min})\right)}, \tag{46}$$

where n_QSO is the number of QSOs in the survey and $z_{i,\min}$ and $z_{i,\max}$ are the limits of the redshift range considered in front of the ith QSO (for example, the one in which DLA lines have been searched for in the given survey, or the redshift range common to the one in which DLA lines have been searched for in a survey and the redshift bin considered).

Table 1
Numerical estimates of the lensing effects for existing DLA surveys. The values were obtained by integrating on L between $L_*/10$ and $10L_*$. For the Lick and LBQS survey, the calculated quantities refer to the redshift range $1.6 < z < 2$.

Quantity	Model	RTB	IUE (whole)	IUE (low domain)	IUE (high domain)	Lick	LBQS
$O_{d\mathcal{N}/dz}$	E	1.08	1.08	1.08	1.18	1.03	1.02
$O_{d\mathcal{N}/dz}$	E+GH	1.19	1.19	1.19	1.43	1.05	1.05
$O_{\Omega_{\rm HI}}$	E	1.19	1.19	1.19	1.43	1.04	1.04
$O_{\Omega_{\rm HI}}$	E+GH	1.34	1.32	1.32	1.79	1.07	1.07

The overdensities are usually small, which can be easily understood: the surveys have characteristics that preclude the signature of strong GL effects. Indeed:

- DLAs are detectable in low S/N spectra of relatively faint QSOs, whose magnitudes are close or larger than the magnitude of the break in the QSO number counts relation: the amplification bias is thus generally inefficient;
- the redshift range in which DLAs are searched for is close to the background QSO redshift, preventing any GL effect to be important. This is systematic in surveys for high-z DLAs conducted from ground-based observatories, as the atmospheric cut-off prevents the detection of DLAs with $z < 1.63$; the presence of Lyman-limit systems in the spectra of a large fraction of even moderate redshift QSOs also contributes to this restriction in surveys for $z < 1.7$ DLAs.

These two facts already indicate that only parts of the $z < 1.7$ surveys may be significantly affected by GL effects, which is better illustrated in Fig. 10 described in the next section. Indeed, the IUE and the RTB surveys searched for DLAs in the redshift ranges which are the most appropriate for lensing (i.e. $z_{\rm DLA} \sim 0.5$ for $z_{\rm q} \gtrsim 1$, or $z_{\rm DLA} \sim z_{\rm q}/2$ for small values of $z_{\rm q}$), and the QSOs used normally have $b_{\rm q} < 16$, necessary for the observations with IUE or for efficient searches of Mg II systems with 4m class telescopes.

Similarly, all high-z surveys may only be marginally affected by lensing: the quasars used for the LBQS survey for DLA systems have an average $b_{\rm q} \simeq 18.3$, while the ones used for the Lick survey have $b_{\rm q} \simeq 18.7$, values which are relatively close to the break in the number counts relations; the mean redshift for the Lick survey QSOs is 2.7 and the one for the LBQS QSOs is 2.2, while all DLAs must have $z > 1.6$ to be detected. As a consequence, we find, for example, that $O_{\Omega_{\rm HI}} > 1.15$ for only about 3% of the total redshift path of the LBQS survey; this value has been evaluated by using redshift intervals of 0.01 and the observed V and $z_{\rm q}$.

The GL effects are larger for the lower redshift surveys. However, in general, we predict that $\Omega_{\rm HI}$ is not overestimated by more than 35% for any of the surveys conducted so far. However, as we shall see below, part of these last two surveys may be more affected.

6.2 $O^{\rm max}$ vs z diagram

A useful representation of the redshift domain in which gravitational lensing may affect a given DLA survey can be constructed in the following way: for each QSO, with known $z_{\rm q}$ and $b_{\rm q}$, one can compute curves like the ones presented in Fig. 8 (or Fig. 6). It is then easy to obtain a quantity which represents the value of the curve maximum (cf. Fig. 6 or Fig. 8). In an $O^{\rm max}_{\Omega_{\rm HI}}$ vs z diagram, as presented in Fig. 10, the black horizontal lines represent the redshift ranges over which DLAs have been searched for in front of QSOs, whose $z_{\rm q}$ appears as a dot on their right; the ordinates of these lines are given by $O^{\rm max}_{\Omega_{\rm HI}}$ which allows to immediately spot the redshift ranges with the strongest lensing effects.

The solid line surrounds the region for which an overdensity $O_{\Omega_{\rm HI}} = \Omega_{\rm HI,GL}/\Omega_{\rm HI,NL} > 1.48$ is computed, which is the value of the quantity $O_{\rm t}$ defined below. This contour line is somewhat irregular, as the redshift domain for which $O_{\Omega_{\rm HI}}$ (or $O_{d\mathcal{N}/dz}$) is larger than a given value changes with $z_{\rm q}$ and $b_{\rm q}$.

Note that the choice of $O^{\rm max}_{\Omega_{\rm HI}}$ over the whole redshift range $0 < z < z_{\rm q}$ is especially appropriate for $z < 1.7$ DLA surveys. A similar diagram drawn for the study of lensing effects in another redshift range (say $1.6 < z < 2$) would strongly benefit in using $O_{\Omega_{\rm HI}}(z = 1.6)$ rather than $O^{\rm max}_{\Omega_{\rm HI}}$. Such a diagram naturally leads to create two distinct tests to check whether GL affects a given survey.

We first divide the observed combined absorber redshift domain in two, named high and low overdensity ones: the *high* overdensity domain covers the domain in redshift for which the overdensity $O_{\Omega_{\rm HI}}$ is larger than a given threshold $O_{\rm t}$; the *low* overdensity domain covers the domain in redshift for which $O_{\Omega_{\rm HI}} < O_{\rm t}$. The value of $O_{\rm t}$ must be such that (condition A) the total redshift paths of the two sub-domains have similar redshift coverages in order to avoid problems

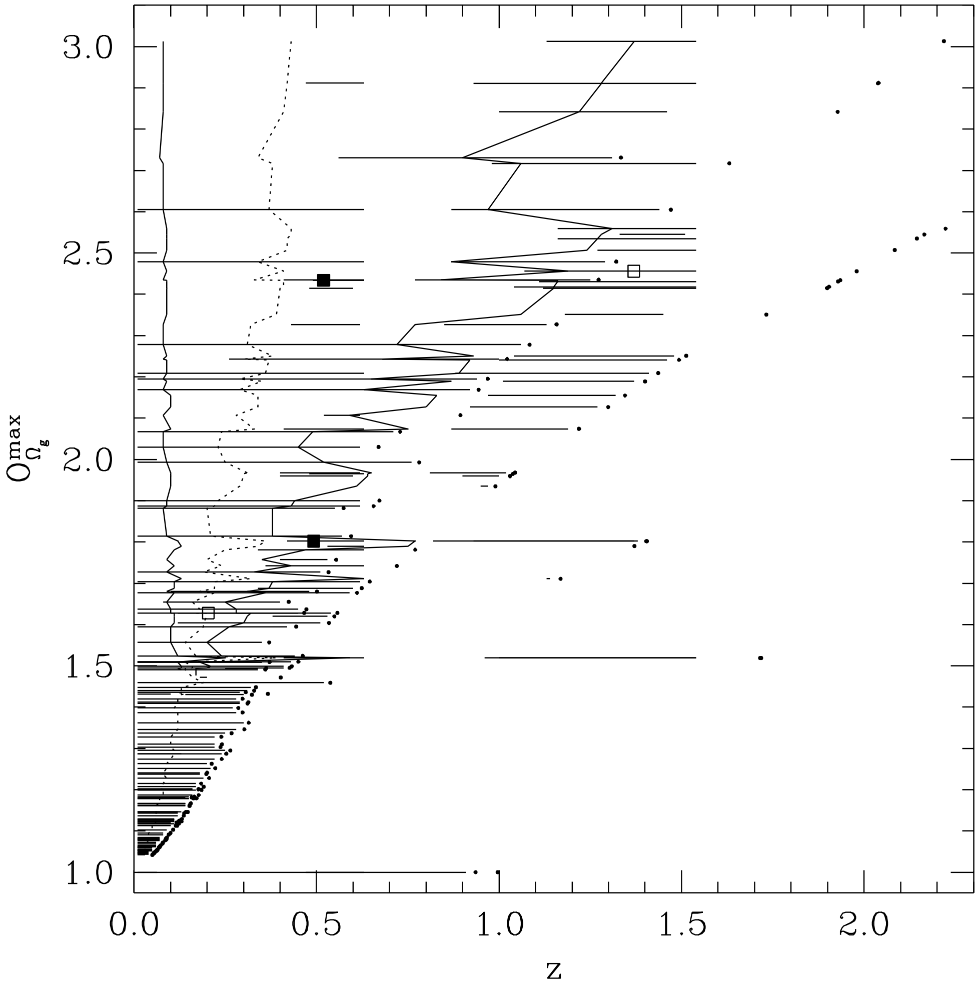

Fig. 10. $z_{\rm abs}$ - $O^{\rm max}_{\Omega_{\rm HI}}$ diagram for the IUE survey obtained with the E+GH model: the horizontal solid lines represent the redshift ranges over which DLAs have been searched for in front of QSOs whose $z_{\rm q}$ appears as a dot on their right. The solid line surrounds the region for which $O^{\rm max}_{\Omega_{\rm HI}} > 1.48$. The squares represent the observed DLAs; they are filled if $\log N_{\rm HI} > 20.6$. The dotted line indicates the redshifts of $O^{\rm max}_{\Omega_{\rm HI}}$ for each QSO.

linked to intrinsic evolution of the absorbers. One may additionally request (condition B) that they have identical total redshift paths. Meeting these two conditions automatically allows one to have very similar values for the total absorption distance paths of the two domains.

For the IUE sample, we had to restrict the absorber redshift domain to $0.15 < z < 0.8$ in order to fulfill condition A. Requesting condition B leads to $O_{\rm t} = 1.48$, so that both the low and high overdensity domains have a total redshift path of $\Delta z_{\rm low} \simeq \Delta z_{\rm high} \simeq 10.3$ and a total absorption distance path of $\Delta X_{\rm low} \simeq \Delta X_{\rm high} \simeq 12.3$; the mean redshift in each domain is $\bar{z}_{\rm low} \simeq \bar{z}_{\rm high} \simeq 0.387$.

It is then remarkable that 3 of the 4 observed DLAs (squares) in the IUE survey indeed appear in the high overdensity domain, and furthermore, that these 3 DLAs are the only ones in the range $0.15 < z < 0.8$. This is even more surprising if one recalls that, at $z = 1.25$, the number density of DLA systems can be expected to be as high as 2.5 times the one at $z = 0.5$, for the evolution parameter $\gamma = 2.27$ (RTB).

We can thus wonder if there is a statistically significant excess of DLAs in the high overdensity domain relatively to the low one and how the determination of the distribution of column densities or the derived value of $\Omega_{\rm HI}$ is also affected.

6.3 Is there an excess of DLAs due to lensing?

We saw earlier that our model predicts at best a 90% excess of DLAs. We find that the 3 confirmed DLAs in the $0.15 < z < 0.8$ range of the IUE survey fall in the high overdensity domain, while there is none in the low overdensity one. Assuming that the redshifts of DLAs follow a Poisson distribution, we can derive the probability to obtain the observed configuration.

Using the number density law given by Eq. 7, the probability to observe $n_{\mathcal{D}}$ DLAs in a domain $\mathcal{D}$ is given by:

$$P(n_{\mathcal{D}};\mathcal{D}) = \frac{(\mu_{\mathcal{D}})^{n_{\mathcal{D}}}}{n_{\mathcal{D}}!}\ \exp\left(-\mu_{\mathcal{D}}\right), \tag{47}$$

with

$$\mu_{\mathcal{D}} = \sum_{i=1}^{n_{\rm QSO}} \int_{z_{i,\rm min}}^{z_{i,\rm max}} \left(\frac{d\mathcal{N}}{dz}\right)_0 (1+z)^{\gamma}\ dz, \tag{48}$$

where $z_{i,\rm min}$ and $z_{i,\rm max}$ are the limits of the redshift range common to the one in which DLAs have been searched for in front of the ith QSO and the one included in the domain $\mathcal{D}$. The probability to observe $n_{\rm low}$ DLAs in the domain low and $n_{\rm high}$ DLAs in the domain high is then given by:

$$P(n_{\rm low}, n_{\rm high}; {\rm low}, {\rm high}) = P(n_{\rm low}; {\rm low})\ P(n_{\rm high}; {\rm high}). \tag{49}$$

Table 2 summarizes the results. It indicates that gravitational lensing is likely to affect the IUE survey as the probability to observe 3 DLAs in the domain high is $\leq 4\%$; the combined probability to observe 3 DLAs in the domain high and none in the domain low is inferior to 2%, and is only 0.3% if the number density of DLAs at $z = 0$ is fixed to the one derived from the observed cross-section of galaxies (RTB).

Table 2
Probabilities
$P_l = P(n_{\rm low}; {\rm low})$, $P_h = P(n_{\rm high}; {\rm high})$ and $P_c = P(n_{\rm low}, n_{\rm high}; {\rm low, high})$ for the IUE and RTB surveys. The values of $\mu_{\mathcal{D}}$ were obtained using Eq. 48 for the IUE survey and Eq. 50 for the RTB survey. The column Ref gives the reference to the values of $(d\mathcal{N}/dz)_0$ and γ necessary to derive $\mu_{\rm low}$ and $\mu_{\rm high}$.

Survey	Ref	$\mu_{\rm low}$	$\mu_{\rm high}$	P_l	P_h	P_c
IUE	LBQS	0.82	0.82	44%	4%	1.8%
IUE	RTB	0.33	0.33	72%	0.4%	0.3%
RTB	LBQS	2.53	2.03	25%	9.3%	2.3%
RTB	RTB	1.42	0.96	24%	1.3%	0.3%

The only fact that two of the 3 DLAs have $N_{\rm HI} > 6\ 10^{20}$ cm^{-2} may also be indicative of GL effects, as one otherwise expects to have a larger number of $2\ 10^{20} < N_{\rm HI} < 6\ 10^{20}$ cm^{-2} DLAs. Furthermore, we find a correlation between $\log N_{\rm HI}$ and $f_{\rm GL}(N_{\rm HI})/f_{\rm NL}(N_{\rm HI})$ for the DLAs and other high $N_{\rm HI}$ systems in the whole IUE sample. We obtain a Kendall (Spearman) Rank-Order coefficient of 0.54(0.67) with a probability of 1.4 % (1.7 %) to exceed this value under the null hypothesis (of no correlation). This latter result is mainly produced by the fact that the two DLAs with $N_{\rm HI} > 6\ 10^{20}$ cm^{-2} are also the ones for which the largest value of $f_{\rm GL}(N_{\rm HI})/f_{\rm NL}(N_{\rm HI})$ is expected.

The RTB survey provides a sample of 43 Mg II system redshifts (their Table 1) instead of the observed redshift domains. We used the assumption – implicit in their study, but not necessarily justified – that the ratio between the cross-section for a DLA absorber and for a Mg II system is independent of z in the absence of significant lensing effects. Hence, we can define O_t to split the survey in 2 sub-samples with equal numbers of Mg II systems: the value $O_t = O_{\Omega_{\rm HI}} = 1.38$ leads to a low overdensity domain with $k_{\rm low} = 22$ Mg II systems at a mean redshift of $\bar{z}_{\rm low} = 0.90$, and a high overdensity domain with $k_{\rm high} = 21$ systems whose mean redshift is $\bar{z}_{\rm high} = 0.63$, somewhat smaller than $\bar{z}_{\rm low}$. We find a larger number of DLAs or candidate DLAs in the high overdensity sample ($n_{\rm high} = 4$, including the 2 confirmed systems) than in the low one ($n_{\rm low} = 2$).

The probability to observe this configuration can be obtained in the same way as previously, if we estimate $\mu_{\mathcal{D}}$ in each domain $\mathcal{D}$ with the following relation:

$$\mu_{\mathcal{D}} = \frac{d\mathcal{N}}{dz}(\bar{z}_{\mathcal{D}})\ k_{\mathcal{D}}, \qquad (50)$$

where $k_{\mathcal{D}}$ is the number of Mg II systems in the domain $\mathcal{D}$ and $\bar{z}_{\mathcal{D}}$ is their mean redshift.

As can be seen in Table 2, we also find good indication that gravitational lensing affects the RTB survey, with a probability of 2.3% or less to obtain the observed configuration. When the determination of the $N_{\rm HI}$ for these candidates becomes available, these probabilities shall increase as some of them will probably not be confirmed as DLA lines.

Nothing prevents us to combine the results obtained from these 2 surveys, although definite conclusions shall also await the confirmation of DLA candidates found by RTB. Using the values of the parameters γ and $(d\mathcal{N}/dz)_0$ given by Wolfe et al. (1995), the combined probability to observe such a configuration in the two samples is 4 10^{-4}; similarly, the values from the RTB survey leads to a combined probability of 9 10^{-6}!

These results indicate that gravitational lensing affects the number density of DLAs in the $z < 1$ surveys.

6.4 Is the derived value of $\Omega_{\rm HI}$ influenced by lensing?

For the E+GH (E) column density profile, the lensing model described here predicts that $\Omega_{\rm HI}$ is only overestimated by 32 % (19%) over the whole IUE survey, and 32% (19%) and 79% (43%) in the low and high overdensity domains, respectively. The relatively small value of the overdensity in the high domain is of course due to the fact that the spectral domain in which DLAs have been searched for is relatively small in the range $0.15 < z < 0.8$ for the QSOs with large $O^{\rm max}_{\Omega_{\rm HI}}$; this is partly explained by the presence of Lyman-limit systems in their spectra.

Unfortunately, due to the few DLAs in the IUE survey, we do not expect to detect a significant lensing effect. However, for the sake of exercise and assuming $q_0 = 1/2$, we find that $\Omega^{\rm obs}_{\rm HI} = 1.33\ h^{-1}\ 10^{-3}$ in the high domain; this value was obtained by inserting the column densities of the 3 detected DLAs in Eq. 11. On the other hand, there is only one large column density system in the low domain for which $N_{\rm HI} = 10^{20.1}$ cm^{-2}; this is thus to low to qualify the system as a DLA. However, inserting this value in Eq. 11 leads to $\Omega^{\rm obs}_{\rm HI} = 0.98\ h^{-1}\ 10^{-4}$ in the low domain. Hence, we find a factor of 13 between the estimates of $\Omega_{\rm HI}$ in the 2 domains; the value in the high sample is ~ 4.7 times the value obtained by LWT for the whole IUE sample. However, no meaningful error bars can be derived which limit the interpretation of this result and also stress for the need of more data.

If even a fraction of this overdensity is confirmed, then our lensing model may not be sufficient to account for it. In this case, the value of $\Omega_{\rm HI}$ for the whole IUE survey may be severely over-estimated because of gravitational lensing, which would mean that its present value may have already been reached by $z \sim 0.7$.

The RTB survey does not provide estimates for the $N_{\rm HI}$ of the DLA candidates. For indication, we present in Table 3 the expected overdensities of DLAs with column densities larger than $N_{\rm inf}$, for different values of $N_{\rm inf}$: for 3 of them, the probability of having a DLA with $\log N > 21.5$ is multiplied by a factor larger than 2!

Table 3
Overdensities ($\int_{N_{\rm inf}}^{\infty} f_{\rm GL}(N)dN / \int_{N_{\rm inf}}^{\infty} f_{\rm NL}(N)dN$) of DLAs with $\log N_{\rm inf} = 20.3, 21.0$ and 21.5 computed for the DLA candidates found in the Rao, Turnshek & Briggs (1995) survey. The values were calculated using the E+GH model.

Name	$z_{\rm q}$	V	$z_{\rm DLA}$	$\log N_{\rm inf} =$		
				20.3	21.0	21.5
$0117+213$	1.491	16.1	0.5761	1.56	2.53	3.51
$0151+045$	0.404	16.9	0.1602	1.21	1.47	1.96
$0302-223$	1.409	16.4	1.0096	1.15	1.34	1.79
$0454+039$	1.343	16.5	0.8596	1.22	1.52	2.15
$1247+267$	2.041	15.6	1.2232	1.26	1.65	2.68
$1622+239$	0.927	17.5	0.4720	1.26	1.59	1.89

Note that the systems for which O is large also indicate that the background quasar may be multiply imaged: this is the case for most of the QSOs which appear in Table 3 (especially 0117+213) and the QSOs 1329+412, 2112+059 and 2223-052 from the IUE survey. HST direct imagery (in the (near-)infrared, as the secondary lensed image is likely to be found very close to the nucleus of the spiral galaxy) of such objects offers the possiblity to confirm the multiply imaged nature of some of these QSOs, which in turn provides unique means for determining the masses of the galaxies giving rise to the DLAs.

7 Conclusions

Assuming that DLAs arise in the disks of spiral galaxies, we have developed a formalism to compute the expected effects (by-pass and amplification bias) of GL on the observed number density of DLAs as a function of redshift. The by-pass effect decreases the effective cross-section for DLA absorption. The amplification bias leads to preferentially selected QSOs whose LOS impact parameter is close to the Einstein radius of the intervening galaxy: it dominates the combined effect for QSOs brighter than $b_{\rm q} = 19$ when evaluating the consequences on the determination of $f(N)$, $d\mathcal{N}/dz$ and $\Omega_{\rm HI}$.

We used two very different column density profiles to characterize the column density distribution within the spiral disks: an exponential (E) and an exponential plus a Gaussian hole (E+GH). We find that the lensing effects are stronger by a factor of ~ 2 in the latter, more realistic, case.

Because of the observational strategy used to search for high-z DLAs, we find that the influence of GL effects is not significant: indeed, only low S/N spectra are necessary which thus allows to use relatively faint $b_{\rm q} \simeq 18.5$ quasars, i.e. with magnitudes close to the break in the QSO number counts. Furthermore, most of the DLAs are searched for in redshift ranges just slightly smaller than the QSO redshifts. Our model leads to conclude that the overestimate of $\Omega_{\rm HI}$ is $> 15\%$ only for 3% of the total redshift path of the LBQS survey; similarly, the overestimate of $\Omega_{\rm HI}$ in the low-z DLA surveys should be at most 35%.

On the other hand, strong effects may actually be seen in surveys ideally designed for lensing, i.e. when searching for $z \sim 0.5$ DLAs in the spectra of bright distant QSOs. Indeed, for $b_{\rm q} \simeq 16$, $z_{\rm q} > 1$ QSOs, DLA surveys lead to over-estimate by up to $\simeq 90\%$ the number of DLAs per unit redshift; to bias the survey towards high H I column density systems so that it may contain up to 4 times as many such systems; thus to overestimate by up to 170% the cosmological density of gas associated with DLAs. Furthermore, the identification of the galaxies responsible for the DLAs may be severely biased towards luminous ones if $2/\alpha_{\rm TF} - \alpha_{\rm H} > 0$; this effect is greatly increased for $\log N_{\rm HI} > 21$ DLAs, so that we expect a 12% or more overdensity of $L > L_*$ galaxies producing $z \simeq 2$ DLAs in front of bright, higher z QSOs, for $\alpha_{\rm H} = 5/12$ and $\alpha_{\rm TF} = 2.6$.

The theoretical results we have presented show that the potential effects of gravitational lensing on the quantities derived from surveys for $z \sim 0.5$ DLAs are of the same order as the ones due to obscuration by dust (Fall & Pei 1993, Pei & Fall 1995), but in the opposite direction. However, combining the two effects in a consistent way may sometimes lead to counter-intuitive consequences, in the sense that a sample of quasars which suffer from extinction by dust is also likely to be subjected to large gravitational effects. We intend to coherently include the effect of dust and micro-lensing on the estimates presented here in a subsequent paper.

We devised some statistical tests to search for the signature of GL in existing DLA surveys, assuming that extinction by dust and micro-lensing effects are negligible. The number of DLAs found in the low-z surveys is too small for definite conclusions to be drawn. However, we find indication that GL is actually at work, from both the effects on the number density and on $\Omega_{\rm HI}$ at low redshifts.

We have exposed a number of limitations inherent to our model, which may be important to explore if the strong lensing effects at $z \sim 0.5$ are indeed confirmed by new data.

During the course of this study, we became aware of a similar work conducted by Bartelmann & Loeb. However, their derivation contains a fundamental error which undermines some of their main results and conclusions.

Acknowledgement

AS thanks M. Franx and F. Briggs for helpful discussions. We are grateful to M. Fall for his useful comments at critical times during the writing of this paper. AS thanks the financial support under grant no. 781-73-058 from the Netherlands Foundation for Research in Astronomy (ASTRON) which receives its funds from the Netherlands Organisation for Scientific Research (NWO). JS thanks the FNRS (Belgium) for a travel grant. JS and JFC have been partially supported by PRODEX.

References

[1] Bar-Kana, R. 1996, ApJ 468, 17

[2] Bartelmann, M., Loeb, A. 1996, ApJ 457, 529

[3] Borgeest, U., Linde, J. V., Refsdal, S. 1991, A&A 251, L35

[4] Briggs, F. H., Wolfe, A. M., Liszt, H. S., Davis, M. M., Turner, K. L. 1989, ApJ 341, 650

[5] Broeils, A. H., van Woerden, H. 1994, A&AS 107, 129

[6] Claeskens, J. F., Jaunsen, A. O., Surdej, J. 1996, in IAU Symposium 173 'Astrophysical Applications of Gravitational Lensing', C. S. Kochanek, J. N. Hewitt (eds.), Kluwer, p. 13

[7] Fall, S. M., Pei, Y. C. 1993, ApJ 402, 479

[8] Foltz, C. B., Chaffee, F. H., Wolfe, A. M. 1988, ApJ 335, 35

[9] Fukugita, M., Turner, E. L. 1991, MNRAS 253, 99

[10] Gott, J. R., Gunn, J. E. 1974, ApJ 190, L105

[11] Hartwick, F. D. A., Schade, D. 1990, Ann. Rev. Astr. Astrophys. 28, 437

[12] Hawkins, M. R. S., Véron, P., 1995, MNRAS 275, 1102

[13] Hewitt, J. N., Haynes, M. P., Giovanelli, R. 1983, AJ 88, 272

[14] Holmberg, E. B. 1975, in 'Galaxies and the Universe', eds. A. Sandage, M. Sandage & J. Kristian, Chicago University Press, p. 151

[15] King, L. J., Browne, I. W. A., Wilkinson, P. N., Patnaik, A. R. 1996 in IAU Symposium 173 'Astrophysical Applications of Gravitational Lensing', C. S. Kochanek, J. N. Hewitt (eds.), Kluwer, p. 191

[16] Lanzetta, K. M., Wolfe, A. M., Turnshek, D. A., Lu, L., McMahon, R. G., Hazard, C. 1991, ApJSS, 77, 1

[17] Lanzetta, K. M., Wolfe, A.M., Turnshek, D. A. 1995, ApJ 440, 435 (LWT)

[18] Milgrom, M. 1988, A&A 202, L9

[19] Pei, Y.C., Fall, S.M. 1995, ApJ 454, 69

[20] Prochaska, J. X., Wolfe, A. M. 1996, ApJ 470, 403

[21] Rao, S. M., Briggs, F. H. 1993, ApJ 419, 515

[22] Rao, S. M. 1994, Ph.D. Thesis, University of Pittsburgh

[23] Rao, S. M., Turnshek, D. A., Briggs F. H. 1995, ApJ 449, 488 (RTB)

[24] Refsdal, S., Surdej, J. 1994, Reports on Progress in Physics 56, 117

[25] Roberts, M. S. 1975, in 'Galaxies and the Universe', A. Sandage, M. Sandage, Kristian, J. (eds.), University of Chicago Press, Chicago, p. 309

[26] Sacket, P.D. 1996, in IAU Symposium 173 'Astrophysical Applications of Gravitational Lensing', C.S. Kochanek, J.N. Hewitt (eds.), Kluwer, p. 165

[27] Schechter, P. 1976, ApJ, 203, 297

[28] Smette, A. 1995, in ESO workshop on QSO absorption lines, Eds G. Meylan et al., Springer-Verlag, p. 275

[29] Smette, A., Robertson, J. G., Shaver, P. A., Reimers, D., Wisotzki, L., Köhler, Th. 1995, A&AS 113, 199

[30] Smette, A., Williger, G. M., Robertson, J. G., Shaver, P. A. 1996, in IAU Symposium 173 'Astrophysical Applications of Gravitational Lensing', C. S. Kochanek, J. N. Hewitt (eds), Kluwer, p. 103

[31] Smith, H. E., Junkkarinen, V. T., Burbidge, E. M. 1977, ApJ 218, 611

[32] Surdej, J. 1990, in "Lecture Notes in Physics, Gravitational Lensing", proceedings of the Toulouse workshop on "Gravitational Lenses", September 1989; Y. Mellier, B. Fort, G. Soucail (eds.), Springer-Verlag, vol. 360, 57-72

[33] Surdej, J., Claeskens, J.-F., Crampton, D., et al. AJ 105, 2064

[34] Tully, R. B., Fisher, J. R., 1977, A&A 54, 661

[35] Tytler, D., 1987, ApJ 321, 49

[36] Véron-Cetty, M., Véron, P. 1991, ESO Scientific Report 10

[37] Wolfe, A. M., Turnshek, D. A., Smith, H. E., Cohen, R. D. 1986, ApJSS, 61, 249

[38] Wolfe, A. M. 1988 in QSO absorption lines: probing the Universe , eds J. C. Blades, D. A. Turnshek and C. A. Norman, Cambridge University Press, p297

[39] Wolfe, A. M., Fan, X. M., Tytler, D., Vogt, S. S., Keane, M. J., Lanzetta, K.M. 1994, ApJ 435, L101

[40] Wolfe, A. M., Lanzetta, K. M., Foltz, C. B., Chaffee, F. H. 1995, ApJ 454, 698 (LBQS)